

A MODEL FOR THE VORTEX PAIR
ASSOCIATED WITH A JET IN A CROSS FLOW

William L. Sellers III

March, 1975

(NASA-CR-136756) A MODEL FOR THE VORTEX PAIR ASSOCIATED WITH A JET IN A CROSS FLOW
M.S. Thesis (Florida Univ.) 87 p HC \$4.75
CSCL 20D
N75-17611
Unclas
G3/34 11961



A MODEL FOR THE VORTEX PAIR ASSOCIATED
WITH A JET IN A CROSS FLOW

By

WILLIAM L. SELLERS III

A THESIS PRESENTED TO THE GRADUATE COUNCIL OF
THE UNIVERSITY OF FLORIDA
IN PARTIAL FULFILLMENT OF THE REQUIREMENTS FOR THE
DEGREE OF MASTER OF SCIENCE

UNIVERSITY OF FLORIDA

1975

ACKNOWLEDGEMENTS

Financial support for this study was provided by NASA Grant NGR 10-005-127 under the technical direction of Mr. R. J. Margason, NASA Langley Research Center, Hampton, Virginia. The author wishes to express his deepest appreciation to Dr. Richard L. Fearn, whose guidance and friendship over the past few years, was instrumental in making this thesis possible. A special note of thanks is given to the author's friends, Robert Weston, Pranab Saha and William Dietz, for their assistance in the completion of this thesis. The author also wishes to thank his wife, Bonnie, whose moral support and assistance during the preparation of this thesis was inestimable.

TABLE OF CONTENTS

Acknowledgements	ii
List of Figures	iv
Symbols	vi
Abstract	viii
Introduction	1
Literature Review	3
Effect of Varying γ_0 in Diffuse Model	12
Extension of Diffuse Model	16
Uncertainty in Extended Model	23
Summary and Conclusions	26
Figures	27
Table I	53
Appendix	55
References	76
Biographical Sketch	77

LIST OF FIGURES

1. Sketch of VTOL Aircraft Transitioning from Hovering to Forward Flight
2. Sketch of Jet Wake Region with Vortex Centers
3. Sketch of Jet Centerline and Vortex Curve with Coordinate Systems
4. Typical V_v Distributions in the $Z_v - Y_v$ Plane
5. Geometry of Vortex Model
6. Comparison of Measured and Calculated Velocity Fields for Cross Section at $X/D = 8.3$ and $R = 8$
7. Standard Deviation versus γ_o , $R = 8$
8. Standard Deviation versus γ_o , $R = 8$
9. Upwash Velocities along Symmetry Plane ($R = 8$, $X/D = 8$, $U_\infty = 127$ ft/sec)
10. Variation of Vortex Strength with γ_o , $R = 8$
11. Variation of Effective Vortex Spacing with γ_o , $R = 8$
12. Variation of Vortex Core Size with γ_o , $R = 8$
13. Variation of Vortex Spacing with γ_o , $R = 8$
14. Vortex Core Size, $R = 8$
15. Options for Vortex Spacing
16. Summary of extended model, $A = 0.72$
17. Vortex Spacing, $R = 8$
18. Effective Vortex Strength, $R = 8$
19. Effective Vortex Spacing, $R = 8$

20. Uncertainty in Vortex Core Size, Equation (14), $R = 8$
21. Uncertainty in Vortex Spacing, Option (1a), $R = 8$
22. Uncertainty in Effective Vortex Strength, Option (1a), $R = 8$
23. Uncertainty in Effective Vortex Spacing, Option (1a), $R = 8$
24. Uncertainty in Vortex Spacing, Option (2a), $R = 8$
25. Uncertainty in Effective Vortex Strength, Option (2a), $R = 8$
26. Uncertainty in Effective Vortex Spacing, Option (2a), $R = 8$

SYMBOLS

A	constant defined by equation (10)
B	constant defined by equation (14)
C	constant defined by equations (15) and (16)
C_1, C_2	constant defined by equations (15a) and (16a)
D	diameter of jet orifice
$\hat{e}_{\theta_1}, \hat{e}_{\theta_2}, \hat{e}_{z_v}$	unit vectors, see figure 5
h_o	half spacing of vortex centers for the diffuse vortex model
R	effective velocity ratio
r, r_1, r_2	distances in vortex coordinate system, see figure 5
r_c	radius of vortex core defined by equation (9)
s	arc distance along vortex curve
U_∞	speed of cross flow fluid
U_v, V_v, W_v	velocity components in vortex coordinate system
X, Y, Z	wind tunnel coordinate system (Cartesian), see figure 3
X_v, Y_v, Z_v	vortex coordinate system (Cartesian), see figure 3
β	diffusion constant, see equation (2)
Γ_o	integrated strength of each diffuse vortex defined by equation (4)
Γ	effective strength of each diffuse vortex, or strength of a vortex filament defined by equation (5)
γ_o, γ	dimensionless variables corresponding to Γ_o and Γ .
$\theta, \theta_1, \theta_2$	angles in vortex coordinate system, see figure 5

σ	standard deviation
σ_w	percent standard deviation defined by equation (12)
ϕ_v	angle between Z and Z_v axis
ω_0	maximum vorticity of each diffuse vortex
ω	vorticity

Abstract of Thesis Presented to the Graduate Council
of the University of Florida in Partial Fulfillment of the Requirements
for the Degree of Master of Science

A MODEL FOR THE VORTEX PAIR ASSOCIATED
WITH A JET IN A CROSS FLOW

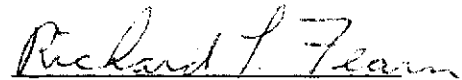
By

William L. Sellers III

March, 1975

Chairman: Richard L. Fearn
Major Department: Engineering Sciences

A model is presented for the contrarotating vortex pair that is formed by a round, turbulent, subsonic jet directed normally into a uniform, subsonic cross flow. The model consists of a set of algebraic equations that describe the properties of the vortex pair as a function of their location in the jet plume. The parameters of the model are physical characteristics of the vortices such as the vortex strength, spacing and core size. These parameters are determined by velocity measurements at selective points in the jet plume.



Chairman

INTRODUCTION

An interesting aerodynamic problem occurs when a vertical takeoff and landing aircraft transitions from hovering to forward flight. The cross flow caused by the aircraft's forward flight interacts with the aircraft's lifting jets, and brings about a loss of performance in addition to stability problems. Figure 1 is a sketch of a VTOL aircraft with a single lifting jet transitioning from hovering to forward flight. The interference between the lifting jet and the cross flow induces a low pressure region in the jet wake and a distribution of pressure induced forces over the aircraft as indicated schematically in the figure. The flow field associated with a VTOL aircraft and its multiple lifting jets is very complex. In order to simplify the problem, while still retaining the essential characteristics of the jet and cross flow interaction process, it has been customary to restrict the problem to that of a single, subsonic jet exhausting normally through a flat plate into a uniform, subsonic cross flow. Other applications of the jet in a cross flow are the cooling of jet turbine combustors, where coolant gases are injected into the combustors to dissipate heat, and the environmental problem of the discharge of cooling water from a power plant into a waterway.

Early investigations into the jet in a cross flow were concerned with a qualitative description of the flow. Several of these investigations resulted in empirical equations for the jet centerline, which was defined to be the locus of maximum velocity in the symmetry plane.

Many of the flow characteristics, it was found, depended on the jet to cross flow momentum ratio. Several investigators found it convenient to use the square root of the momentum ratio and defined it as the effective velocity ratio. In certain restrictive cases, it was shown that the effective velocity ratio reduced to the jet to cross flow velocity ratio. (ref. 1).

Recently there have been several detailed studies into the velocity and pressure fields associated with the jet in a cross flow. In each of these investigations it was found that the jet wake was dominated by a pair of contrarotating vortices. Kamotani and Greber (ref. 2) and Harms (ref. 3) investigated the effect of heated jets on the flow field. Thompson (ref. 4), utilizing an unheated jet, conducted a study of the pressure distribution on a flat plate and the velocity field induced by a jet in a cross flow. Fearn and Weston (ref. 1 and 5) investigated the velocity and pressure fields associated with an unheated jet directed normally into a cross flow. Fearn and Weston presented simple analytic models for the vortex pair associated with a jet in a cross flow.

This paper will investigate the effect of varying certain parameters in one of the models presented by Fearn and Weston. The vortex model will also be extended to give a more convenient means of determining the vortex properties.

LITERATURE REVIEW

An important feature of the jet in a cross flow is the contrarotating vortices that roll up in the wake region. Figure 2 is a sketch of the wake region induced by a jet in a cross flow. A plane of symmetry ($Y=0$) is seen to exist in the flow field. The vortex centers are defined as the points of maximum vorticity in a cross section and are shown schematically in figure 2. The loci of the vortex centers are commonly referred to as the vortex trajectories. It is convenient to define the projections of the vortex trajectories onto the symmetry plane as the vortex curve, shown schematically in figure 3. The vortex curve is then described as the locus of the midpoints of the line joining the vortex centers. It is seen in figure 3 that the vortex curve falls slightly below the jet centerline. Figure 3 also illustrates the reference frames commonly in use. One reference frame has its origin at the center of the jet exit and is aligned with the tunnel coordinate system. Two other coordinate systems are aligned with cross sections perpendicular to the jet centerline and the vortex curve. The system referred to the jet centerline has its axes denoted with a subscript j while the system referred to the vortex curve has its axes denoted with a subscript v .

Kamotani and Greber (ref. 2), who were prompted by the gas turbine combustor cooling problem, utilized a 1/4 inch diameter jet in their study of heated and unheated jets in a cross flow. The authors found that the flow was dominated by a pair of contrarotating vortices that form behind the jet and persist for a long distance downstream of the

jet orifice. This compares with the findings of Pratte and Baines (ref. 6), in which the vortices were located as far as 1000 jet diameters downstream of the jet orifice. Kamotani and Greber presented the data as plots of velocity and temperature distributions in the symmetry plane and in planes perpendicular to the jet centerline. The vortices were apparent when the velocity vectors in the wake region were projected into cross section planes perpendicular to the jet centerline. Results were shown for effective velocity ratios of 3.91 and 7.72. The authors made no attempt to calculate the strength of the vortex pair.

The aerodynamic problems associated with V/STOL aircraft have motivated several recent papers. Harms (ref. 3) studied the temperature effects on the velocity field induced by a 5 centimeter diameter jet issuing into a cross flow. Extensive velocity measurements were taken in planes perpendicular to the tunnel axis for an effective velocity ratio of 8. It was found that the position of the vortex centers remained essentially the same for hot and cold jets of the same effective velocity ratio. The only difference being that for the hot jet the vortices were more diffuse. Harms stated that the vortex pair absorbed the axial momentum of the jet and were dissipated in the far field by the action of viscous forces. Harms' study was similar to Kamotani and Greber in that he recognized that the vortices were the dominant feature, but no attempt was made to calculate their strength.

Thompson (ref. 4) investigated the ground board pressure distribution and velocity field induced by unheated jets issuing into a cross flow. Thompson utilized a one inch diameter jet, in addition to elliptic

jets of comparable exit area. Velocity measurements were taken in cross section planes perpendicular to the jet centerline.

Thompson attempted to infer the strength and location of the vortices induced by a circular jet for effective velocity ratios of 2, 4 and 8. The vortex centers were located from the distribution of the sidewash component (V_v), of the velocity in cross section planes approximately perpendicular to the vortex curve. The V_v distributions were found by taking velocity measurements in traverses parallel to the Z_v and Y_v axes in the cross section plane. Figure 4a is a sketch illustrating typical V_v distributions in the cross section planes. The V_v component changed sign as the line joining the vortex centers was traversed in a Z_v direction. The vortex separation was determined by locating the peaks in the V_v distribution as the individual vortices were traversed in a Y_v direction. Thompson assumed that the vortex properties changed slowly enough with X_v that the vortices could be treated as though they were two-dimensional. The velocity induced by a single, two-dimensional vortex filament was equal to $\Gamma/2\pi r$, where Γ was the vortex strength and r was the radial distance from the vortex center. Thompson measured the V_v component of velocity in a traverse parallel to the Z_v axis in the cross section and passing through the vortex center. Figure 4b is a sketch of typical velocity distributions determined by this procedure. Plots of $2\pi V_v Z_v$ versus Z_v were made assuming that the curve should asymptote to the value of the vortex strength once a distance had been traversed that was sufficient to account for all the vorticity. Thompson encountered some difficulty with his asymptotic method for calculating the vortex strength. The author found that the entire vorticity field had not been covered inside

the traversed area since the vortices were more diffuse than he expected. The author recognized this fact and stated that the given values for the vortex strengths were low for effective velocity ratios of 6 and 8. Thompson's method assumed the vortices were discrete and the velocity field fell off as $1/r$, as in the single vortex filament. Since the vortices were diffuse, there was interaction between them which would also keep the asymptotic method from approaching the true value of the vortex strength.

Fearn and Weston (ref. 1) conducted a study of the velocity field associated with a jet in a cross flow. The purpose of their study was to relate the velocity field, in cross sections perpendicular to the vortex curve, to the vortex properties through simple analytic models. A four inch diameter, unheated, circular jet directed normally through a 4 ft. by 9 ft. ground board was employed in the experiment. Velocity measurements were taken for effective velocity ratios from 3 to 10 and for a range of downstream distances of 2 to 45 jet diameters. The measurements were taken with a rake of seven yaw-pitch probes that was traversed in cross section planes.

The authors presented two models for the contrarotating vortex pair associated with a jet in a cross flow. Like Thompson, the authors assumed that the vortex properties change gradually in the X_v direction. In both models the vortices were treated as though they were two-dimensional and no attempt was made to account for an axial velocity component. The filament model approximated the vortex pair with two vortex filaments of strength $\pm\Gamma$ and located at $Y_v = \pm h$. The diffuse model assumed a Gaussian distribution of vorticity within each of the

vortices. In both models the projection of measured velocities onto cross section planes were used to infer the location and strength of the vortices at that cross section.

The filament model used measured velocities along the Z_v axis to determine the vortex properties. It was felt that the large upwash velocities (W_v), that occur along the Z_v axis would give the best results in determining the vortex properties. The filament model assumed the velocity in a cross section was the result of the superposition of the free stream component of velocity in the plane of the cross section with the velocity induced by the vortex pair. Reference 1 gave the equation for the upwash velocity along the Z_v axis as

$$W_v = \Gamma h / [\pi(h^2 + Z_v^2)] - U_\infty \sin \phi_v \quad (1)$$

where ϕ_v is the angle between the Z and the Z_v axis. The vortex properties were determined by fitting the measured upwash velocities in a least squares sense to equation (1).

The diffuse model used a large number of measured upwash velocities in a cross section to determine the vortex properties. By fitting the measured upwash velocities in a least squares sense to the equation for the velocity predicted by the model, the strength Γ_0 , spacing h_0 , and diffusivity β , of the two diffuse vortices were determined. Figure 5 illustrates the coordinate system used in the development of the diffuse model. The vorticity ω was assumed to be

$$\omega(r, \theta) = \omega_0 (e^{-\beta^2 r_1^2} - e^{-\beta^2 r_2^2}) \quad (2)$$

where ω_o is the maximum vorticity of each vortex. The velocity at any point in the cross section was assumed to be the result of the superposition of the velocity induced by the vortex distribution given in equation (2) and the component of the free stream velocity in the cross section plane.

$$\bar{v} = \frac{\Gamma_o}{2\pi} \left[\frac{(1-e^{-\beta^2 r_1^2})}{r_1} \hat{e}_{\theta_1} - \frac{(1-e^{-\beta^2 r_2^2})}{r_2} \hat{e}_{\theta_2} \right] - U_\infty \sin \phi_v \hat{e}_{z_v} \quad (3)$$

The integrated strength Γ_o , of a single diffuse vortex was defined to be

$$\Gamma_o = \int_0^{2\pi} \int_0^\infty \omega_o e^{-\beta^2 r^2} r dr d\theta \quad (4)$$

Figure 6 shows the measured velocity vectors projected into a cross section plane together with the velocity predicted by the diffuse model. It is seen that the diffuse model provides an adequate description of these velocities.

The authors were able to obtain several analytic relationships from the model. The effective strength Γ of each diffuse vortex was defined to be the net flux of vorticity across the half plane of the cross section and was given by

$$\Gamma = \int_{-\pi/2}^{\pi/2} \int_0^\infty \omega(r, \theta) r dr d\theta \quad (5)$$

The effective spacing or center of vorticity h , was defined as

$$h = \frac{1}{\Gamma} \int_{-\pi/2}^{\pi/2} \int_0^{\infty} \omega(r, \theta) Y_v r dr d\theta \quad (6)$$

Since diffusion and cancellation of vorticity were expected across the symmetry plane, Γ may be smaller than Γ_0 . The authors pointed out that the effective strength and spacing determined by the diffuse model was assumed to be equal to the strength and spacing determined by the filament model. Equations relating the parameters of the diffuse model were found by evaluating equations (5) and (6). The results were

$$\Gamma = \Gamma_0 \operatorname{erf}(\beta h_0) \quad (7)$$

and
$$h = h_0 / \operatorname{erf}(\beta h_0) \quad (8)$$

where
$$\operatorname{erf}(\beta h_0) = \frac{2}{\sqrt{\pi}} \int_0^{\beta h_0} e^{-t^2} dt$$

is the error function.

The relationship between the diffusivity and the vortex core size r_c , was given by

$$\beta = 1.121/r_c \quad (9)$$

where r_c was defined to be the distance from the vortex center to the point where the maximum tangential velocity occurs. The authors presented most of the data in non-dimensionalized graphical form. The parameters h , h_0 , and r_c were non-dimensionalized by the jet diameter. The strength of the vortices was non-dimensionalized by the quantity $2DU_{\infty}$,

i.e. $\gamma = \Gamma/2DU_\infty$ and $\gamma_0 = \Gamma_0/2DU_\infty$. The quantity $2DU_\infty$ was shown by Chang-Lu (ref. 7) to be equal to the roll up of the vorticity around a two-dimensional cylinder.

The results of the experiment by Fearn and Weston (ref. 1) provided several interesting implications. The authors found the vortex strength was essentially constant for each velocity ratio and could be described in a linear form

$$\gamma_0 = AR \quad (10)$$

where R was the effective velocity ratio. By fitting the data for each velocity ratio separately, the constant was determined to be, $A = 0.72$. The fact that Γ_0 was related to R in a linear manner suggests that Γ_0 was a function of the jet exit velocity and diameter. The authors presented a qualitative description of the vortex system:

The vortex pair is formed very close to the jet orifice with an initial strength that is directly proportional to the speed of the jet at the orifice and to the diameter of the jet. The vortices are deflected by the cross flow and they diffuse at a rate which is a function of the arc length along the vortex curve, but which is a weak function of effective velocity ratio. The vortices gradually weaken each other by diffusion of vorticity across the symmetry plane. (p. 1671)

To summarize, Fearn and Weston were able to predict the velocity field induced by the vortex pair to an adequate degree by the diffuse model. Equations (6) through (9) were obtained relating several of the vortex parameters.

It was later shown by Fearn (ref. 8) that

$$BD \propto (s/D)^{-1/2} \quad (11)$$

where s was an arc length along the vortex curve and D was the jet diameter. This relationship was not without physical significance, in that equation (11) could be related to a "kinematic or eddy" viscosity for turbulent flow.

EFFECT OF VARYING γ_0 IN THE DIFFUSE MODEL

The equation $\gamma_0 = AR$, given by Fearn and Weston, is an important result of their diffuse model. Since the equation will be used in almost any effort to extend the diffuse model, a study is conducted as to its validity. An investigation is made into the procedure for determining the constant A, together with the effect that varying γ_0 has on the vortex properties.

The investigation is performed by varying the value of A in the two-parameter, diffuse model computer program developed by Robert Weston. The program is listed for reference in Appendix 1. The computer program utilizes the method of differential corrections (ref. 9), to fit the measured upwash velocities in a cross section to the Z_v component of equation (3). The computer program sets γ_0 equal to a constant and varies h_0 and β for the best fit, in a least squares sense, to the measured upwash velocities. Once a fit is obtained for a cross section, the program calculates the "quality" of the fit in terms of a standard deviation σ (ref. 10). In this study the computer program calculates the quality of the fit in terms of a percent standard deviation

$$\sigma_w = \frac{\sigma}{V_{\max}} 100 \quad (12)$$

where V_{\max} is the maximum upwash velocity induced by the vortex pair alone. Through an iterative procedure, the program is able to search and find the value of $\gamma_0 = AR$, which corresponds to the minimum σ_w and thus the best fit to the upwash velocities.

In this study only the measured velocity data for an effective velocity ratio of 8 is used since it is the most extensively studied by Fearn and Weston. Figure 7 is a plot of σ_w versus the constant A in $\gamma_0 = AR$. Table 1 contains information showing the size, location, and number of velocity measurements for each cross section in Figure 7. The overall σ_w curve is calculated by fitting the measured upwash velocities for all cross sections together. It is interesting to note from figure 7, that although a minimum point does exist for most of the cross sections, only a cutoff for small values of γ_0 is predicted by the diffuse model. The value of γ_0 can increase indefinitely (increase A) once a certain value of A has been reached, with no significant increase in σ_w . To determine if this trend is a function of the number of velocity measurements in a cross section, the measured velocities from Harms' experiment (ref. 3) are input into the two-parameter, diffuse model program. Table 1 illustrates that one of the cross sections studied by Harms contains more velocity measurements than a similar cross section of Fearn and Weston. Figure 8 shows the σ_w versus A curve that is the result of Harms' measurements. It can be seen in figure 8 that the same large plateau exists in the σ_w curve. It appears that the number of velocity measurements does not change the large plateau in the σ_w curve for increasing γ_0 .

In an effort to gain some insight into why the plateau occurs in the σ_w curves, the manner in which the diffuse model describes the upwash velocities for a range of A is investigated. The upwash velocities predicted by the model are examined for values of A equal to 0.4, 0.72 and 5.0. The cross section at $X/D = 8.3$ is examined since it is the most

extensively studied cross section for an effective velocity ratio of 8. Figure 9 is a plot of the upwash velocities (W_v), versus Z_v along the symmetry plane of the cross section. The upwash velocities are non-dimensionalized by the free stream velocity. Figure 9 shows that the model describes the upwash velocities adequately for values of A equal to 0.72 and 5.0. It is also seen that the model cannot describe the upwash velocities for an $A = 0.4$. Figure 9 infers that a certain value of γ is necessary to describe the upwash velocities and once this value of γ is reached the net flux of vorticity across the half plane remains constant for increasing γ_0 . This is also illustrated in figure 10, which is a plot of γ versus the constant A . For values of $A \geq 1.0$, it is seen that γ remains essentially constant for each cross section.

The plateau in the σ_w curves in figures 7 and 8 can then be explained from

$$\gamma = \gamma_0 \operatorname{erf} (\beta h_0) \quad (7)$$

together with the knowledge of how the vortex properties vary with γ_0 . Figures 10, 11 and 12 illustrate that the properties γ , h and r_c remain essentially constant for $A \geq 1.0$. Figure 13 shows the vortex spacing h_0 decreases rapidly with increasing γ_0 . The diffuse model attempts to keep the value of γ in equation (7) constant by shifting the various vortex parameters. For increasing γ_0 , the term $\operatorname{erf} (\beta h_0)$ in equation (7) must decrease to keep γ constant. The properties r_c or β remain essentially constant while h_0 decreases in such a way that $\operatorname{erf} (\beta h_0)$ decreases to keep γ constant. For decreasing γ_0 , the term $\operatorname{erf} (\beta h_0)$ must increase to keep γ constant. The parameter r_c decreases

(β increases), as the vortices tend toward filaments in an effort to match the upwash velocities. The vortex spacing h_0 also increases, but the term $\text{erf}(\beta h_0)$ asymptotes to a value of one and cannot increase further. The result is that for γ_0 below a certain value, the effective vortex strength γ decreases (figure 10). The vortices are then too weak to describe the measured upwash velocities which causes σ_w to increase.

In summary, this investigation did not find an error in the value of $A = 0.72$ given by Fearn and Weston, since the overall fit for $R = 8$ does have a physical minimum in this region (figure 7). This study does show that any value of $A > 0.6$ will work almost as well.

EXTENSION OF DIFFUSE MODEL

Fearn and Weston present most of the vortex properties in graphical form. It will be more convenient to an aircraft designer if the vortex properties are expressed algebraically as a function of arc length along the vortex curve for a given effective velocity ratio. This study, as stated previously, will consider only the diffuse vortex properties for an effective velocity ratio of 8.

Fearn and Weston (ref. 1) present several equations relating the vortex properties, which are listed again for reference.

$$\gamma = \gamma_0 \operatorname{erf} (\beta h_0) \quad (7)$$

$$h = h_0 / \operatorname{erf} (\beta h_0) \quad (8)$$

$$\gamma_0 = AR \quad (10)$$

In addition, from reference 8 it is found,

$$\beta D \propto (S/D)^{-1/2} \quad (11)$$

It is seen from equations (7), (8), (10) and (11), that 4 equations with 5 unknowns (γ , γ_0 , h , h_0 , β), are available to describe the vortex properties. An additional equation is needed together with an explicit statement concerning equation (11) in order to describe the vortex properties algebraically. Before the projection of velocity field onto

a cross section plane can be reconstructed from the vortex parameters together with equation (3), a description is needed for the vortex curve. Fearn and Weston (ref. 1) present an empirical equation for the vortex curve, which is given by

$$Z/D = a_v R^{b_v} (X/D)^{c_v} \quad (13)$$

where $a_v = 0.3473$, $b_v = 1.127$ and $c_v = 0.4291$. Values of ϕ_v and s/D can then be calculated for a range of X/D .

In this study the two-parameter diffuse model program is used to generate the vortex properties at each cross section for an $A = 0.72$. From equation (9), it is seen that a one to one correspondence occurs between β and r_c . Since the diffusivity β is more difficult to visualize than the core size r_c , the latter will be given in the figures. For convenience, β will be used in determining the vortex properties and converted to r_c through equation (9). Figure 14 is a plot of the vortex core size versus s/D . It is seen that no data is available near the jet orifice ($s/D < 5$), therefore, any empirical equations for r_c or β will be an extrapolation in this region. This will also be true for any additional equations obtained from the results of data presently available. From equation (11), the simplest possible description of β is given by

$$\beta D = \frac{B}{(s/D)^{1/2}} \quad (14)$$

where B is a constant.

The constant B is determined by fitting the values of βD predicted by the diffuse model, in a least squares sense to equation (14). It is noted that equation (14) infers that the vortices approach filaments at the jet exit. Figure 14 shows that the empirical equation gives an adequate description of the vortex core size. Since β (or r_c) is a weak function of the effective velocity ratio, equation (14) will give a fairly reasonable description of β for other effective velocity ratios as well.

To make the system of equations complete, an additional equation is required which does not introduce still another unknown. One possibility is an equation describing the vortex spacing h_o , as a function of s/D . By examining the values of h_o predicted by the diffuse model, two possible options are obtained for the vortex spacing. Both options are based on assumptions for the starting positions of the vortices in the region near the jet orifice. Figure 15 shows the two options and 4 equations that this study will use to describe the vortex spacing.

Figure 15 shows that option 1 assumes the vortices start as two concurrent vortex filaments at the jet exit. Since the contrarotating vortices are concurrent at the jet exit, this model forces the vortex strength to zero at the orifice. Two equations are shown that describe the vortex spacing adequately,

$$\frac{h_o}{D} = C(1 - e^{-\frac{s/D}{K}}) \quad (15)$$

or

$$\frac{h_o}{D} = \frac{s/D}{C_1(s/D) + C_2} \quad (15a)$$

where C , C_1 and C_2 are constants.

Figure 15 shows that option 2 assumes the vortices start as vortex filaments that emerge from the side of the jet orifice. Option 2 gives the possibility of a non-zero vortex strength at the jet orifice and will resemble the qualitative description of the vortices given by Fearn and Weston (ref. 1). The equations describing the vortex spacing are simple modifications of the two previous equations,

$$\frac{h_o}{D} = C(1 - e^{-\frac{s/D}{R}}) + .5 \quad (16)$$

or

$$\frac{h_o}{D} = \frac{s/D}{C_1(s/D) + C_2} + .5 \quad (16a)$$

where C , C_1 and C_2 are constants.

The extended model consists of equations (7), (8), (10) and (14) together with one of the four equations for the vortex spacing. Each option of the extended model is denoted by the equation that is used to calculate h_o . The undetermined constants in the 4 options for the vortex spacing are determined by fitting the values of γ predicted by the diffuse model, in a least squares sense, to the equation for γ obtained from the extended model. Some question may occur over the decision to fit to γ instead of the more straightforward method of fitting to h_o . It is felt that the vortex strength is the most important property and the best description of the strength is obtained by fitting to γ . In addition, a later chapter will show that a large amount of uncertainty exists in the values of h_o predicted by the

diffuse model. A description is given as to how the constant is determined in one of the options. For example option (1a) will calculate the vortex strength γ , from

$$\gamma = AR\text{erf} \left[\frac{B}{(s/D)^{1/2}} C(1 - e^{-\frac{s/D}{R}}) \right] \quad (17)$$

The undetermined constant C is calculated by fitting the values of γ predicted by the diffuse model, in a least squares sense, to equation (17). The constants C , C_1 and C_2 in the other options are found in a similar manner.

Figure 16 is a summary of the extended models for an $A = 0.72$. The figure illustrates all the equations for each option together with values for all the constants. Figures 17 through 19 illustrate how well the different options describe the vortex properties for an $A = 0.72$. Figure 17 shows the vortex spacing h_0 , together with the empirical results from the four options of the extended model. It is seen in figure 17 that there is little difference in options (1a) and (1b). Similarly there is little difference in options (2a) and (2b). It is interesting to note, that for s/D greater than 10, it makes little difference whether the vortices start at the origin (options (1a) and (1b)) or emerge from the side of the jet exit (options (2a) and (2b)). Figure 18 shows that the vortex strength γ , is independent of initial vortex position for s/D greater than 10. It is also seen in figure 18 that γ does depend quite drastically on the initial vortex position for s/D less than 5. No conclusion can be reached on the value of γ near the jet orifice until more data on the vortex strength and spacing

is obtained in this region. Figure 18 also shows the standard deviation σ of each option in fitting to γ . Figure 19 shows that the effective vortex spacing h , is independent of initial vortex position for s/D greater than 4.

To illustrate how the model is used to calculate the vortex properties, a sample calculation will be made with the use of option (1a). For a cross section located at $X/D = 15.23$, a value of $\phi_v = \tan^{-1} [d(Z/D)/d(X/D)]$ can be calculated from equation (13). By a numerical integration of equation (13), a corresponding value of s/D can be obtained. In this manner the values of $\phi_v = 18^\circ$ and $s/D = 20.5$ are obtained. For an s/D of 20.5, the vortex properties are calculated as,

$$\gamma_o = (.72)8 = 5.76$$

$$h_o/D = 2.04(1 - e^{-\frac{20.5}{8}}) = 1.88$$

$$\beta D = 2.11/(20.5)^{1/2} = 0.466$$

$$\gamma = \gamma_o \operatorname{erf}(\beta h_o) = 4.537$$

$$h/D = (h_o/D)/\operatorname{erf}(\beta h_o) = 2.396.$$

The projection of the velocity field onto this cross section plane can then be calculated at any point throughout the cross section from equation (3).

In summary, several options are obtained to extend the diffuse model given by Fearn and Weston. With the use of these options, the vortex properties and the projection of the velocity field onto any cross section plane can be calculated. It is noted however, the

options are extrapolations of available data in the region of the jet orifice. For $s/D > 10$, the vortex properties are adequately described by any one of the four options.

UNCERTAINTY IN EXTENDED MODEL

Since the extended models are the result of curve fitting to the diffuse vortex properties, some insight into the uncertainty of the diffuse vortex properties is necessary. The criteria that are used to set the limits on the uncertainty of the diffuse vortex properties are established with the use of figure 7. As stated previously, the lower cutoff on γ_0 is distinct. For each cross section in figure 7 the lower or percentage cutoff is defined to be the value of the constant A that corresponds to twice the value of σ_w at the minimum of the cross section. The plateau on the σ_w curves raises some question as to a proper cutoff limit for large values of A. Since the constant A can increase indefinitely without a large increase in the value of σ_w , the value of A = 2.0 is arbitrarily chosen. This value of A is sufficiently far out on the plateau that the vortex properties (with the exception of h_0) are not changing rapidly with A. With this criteria established, figures 10 through 13 are used to determine the diffuse vortex properties at the percentage (lower) and plateau (upper) cutoffs. It should be noted that the percentage cutoff will vary from cross section to cross section but the plateau cutoff remains at A = 2.0.

Figure 20 is a plot of the core size from the diffuse model for a constant A = 0.72. The uncertainty bars are shown for each cross section. The bars marked with the double tick mark are the result of the percentage cutoff for each cross section. The bars marked with a

single tick mark are the result of the plateau cutoff. It is necessary to determine if the empirical equation for r_c , equation (14) together with equation (9), will still describe the vortex properties throughout the region of uncertainty. Equation (14) is fit in least squares sense to the values of βD predicted by the diffuse model for constants of A equal to 0.48 and 2.0. These two values of the constant A correspond to the percentage and plateau cutoff as determined from the overall fit for all cross sections in figure 7. These two values of A will then be used to set uncertainty limits on the extended model. Figure 20 shows that the empirical equations will describe the vortex core size adequately in the region of uncertainty.

In the remaining portion of this study, options (1a) and (2a) are used because of their relative simplicity. The diffuse vortex properties shown in figures 21 through 26 are determined from the diffuse model for a constant $A = 0.72$. Figures 21 through 23 show the uncertainty in the diffuse vortex properties together with the empirical descriptions given by option (1a). Figure 21 illustrates that there is a large uncertainty in the vortex spacing h_0 given by the diffuse model. It is also seen in figure 21 that option (1a) still gives an adequate description of the vortex spacing in the region of uncertainty. Figure 22 shows the uncertainty in the effective vortex strength γ , from the diffuse model together with the filament model results (ref. 1). Extended model (1a) is seen to describe the vortex strength adequately and the standard deviation σ , in fitting to γ is given for each curve. Figure 23 shows that there is very little uncertainty in the effective vortex spacing given by the diffuse model. For all but one cross section,

the uncertainty bars remained within the symbol width. There is a discrepancy in that some of the filament model results lie outside of the uncertainty limits of the diffuse vortex properties and the extended model curves. It is believed that at these points an insufficient number of velocity measurements were taken for the filament model to adequately describe the upwash velocity distribution. This will cause the filament model to give unreliable values for the vortex properties.

Figures 24 through 26 are similar to figures 21 through 23 except the empirical curves are determined by option (2a). It is seen in figure 25 that option (2a) encounters difficulty in describing the vortex strength γ , for a constant of $A = 2.0$.

In summary, the extended model will give adequate descriptions throughout the range of uncertainty in the diffuse vortex properties. The one exception is that option (2a) cannot describe the vortex strength for a value of $A = 2.0$.

SUMMARY AND CONCLUSIONS

An investigation is conducted into the diffuse vortex model given by Fearn and Weston (ref. 1). The equation, $\gamma_0 = AR$, presented by the authors, is examined in detail as to the procedure for determining the constant A. As in reference 1, the value of $A = 0.72$ is found to give the best description of the upwash velocities in a cross section for an effective velocity ratio of 8. However, this study has also shown that, in a practical sense, any value of A greater than 0.6 will work almost as well.

The diffuse vortex properties presented by Fearn and Weston, are extended from a graphical to an algebraic description of the vortex properties for an effective velocity ratio of 8. The extended model consists of the analytic equations given in reference 1, together with empirical equations given in this paper. With the use of the extended model, the vortex properties together with the projection of the velocity field in a cross section plane can be calculated for any cross section in the flow. However, in the region near the jet orifice, the extended model represents an extrapolation of available data. The extended model gives an adequate description of the vortex properties for $s/D > 10$. The uncertainty in the results of the extended model is also investigated.

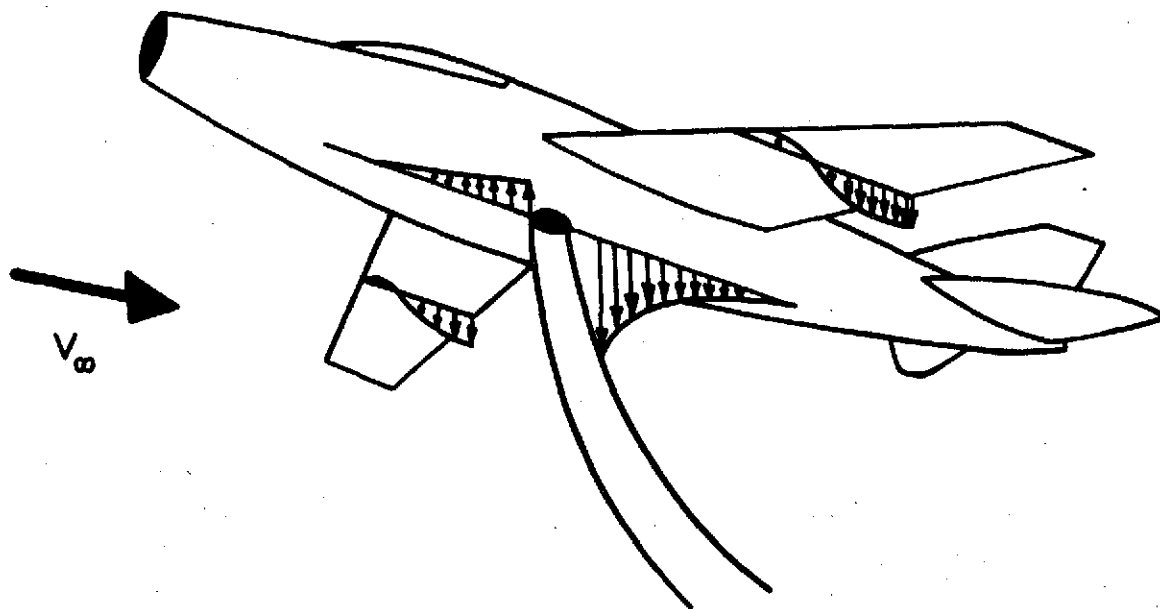


Figure 1. Sketch of VTOL Aircraft Transitioning
from Hovering to Forward Flight

ORIGINAL PAGE IS
OF POOR QUALITY

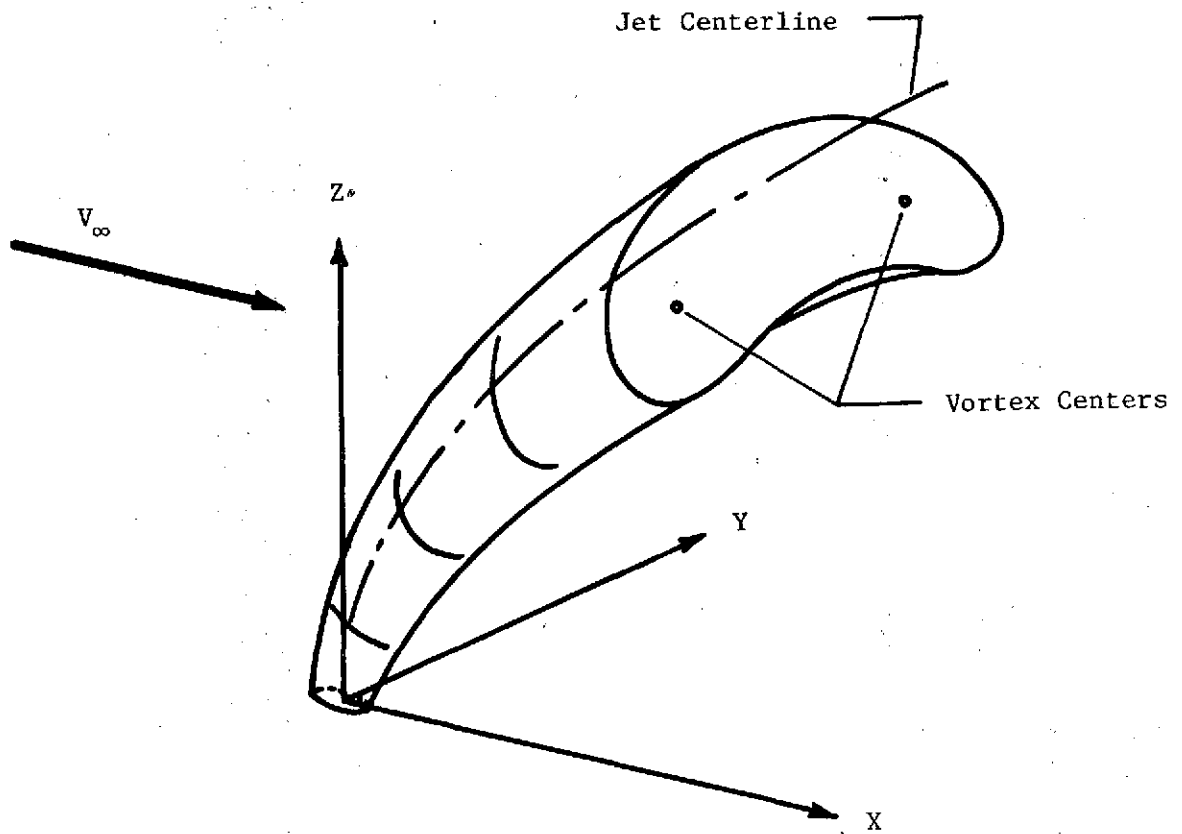


Figure 2. Sketch of Jet Wake Region with Vortex Centers

ORIGINAL PAGE IS
OF POOR QUALITY

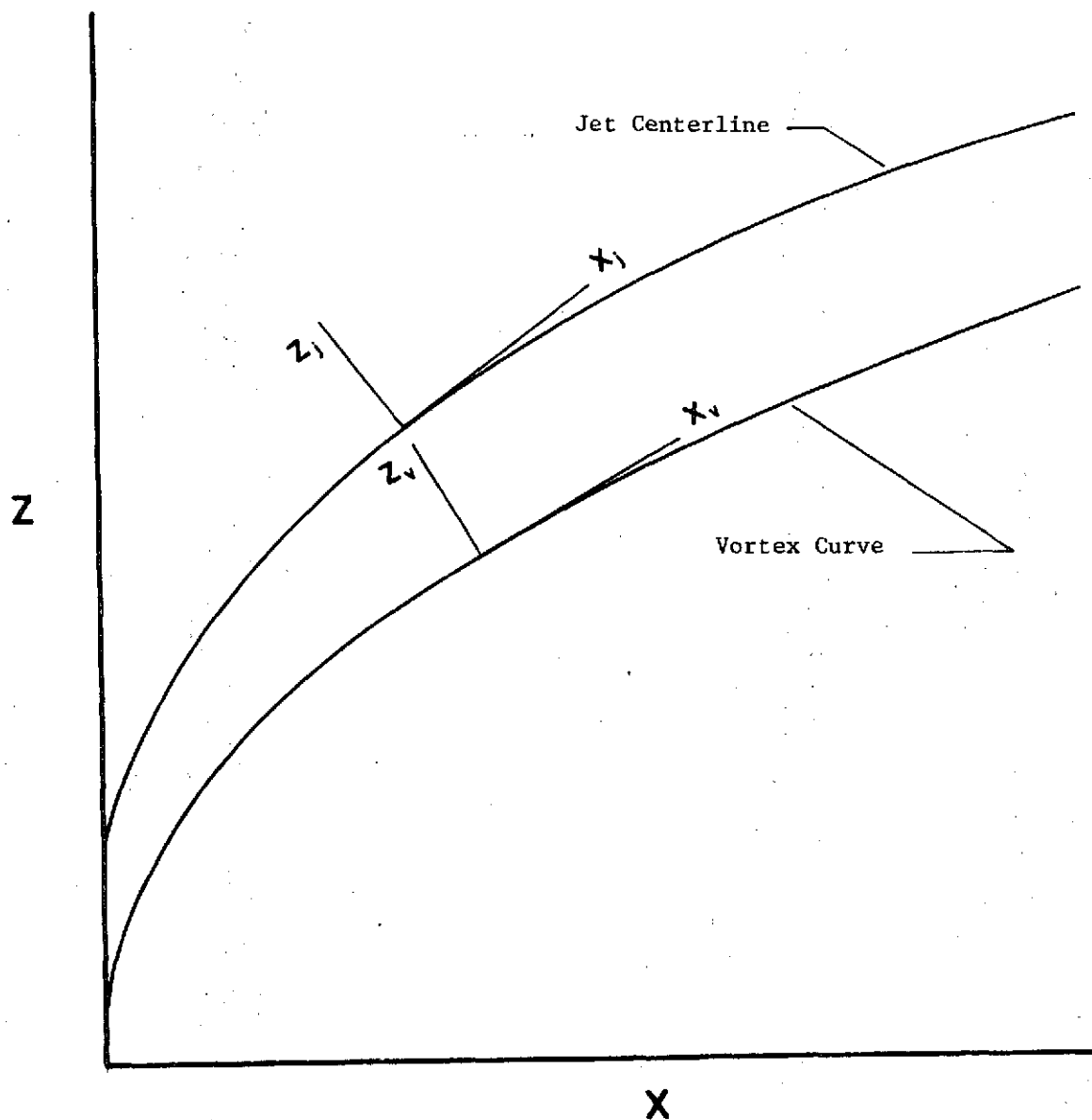
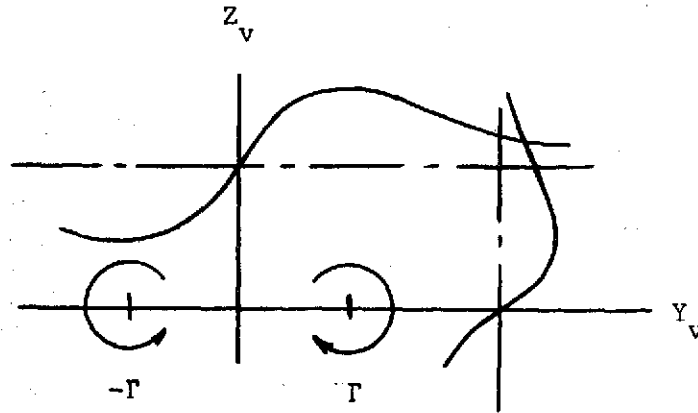
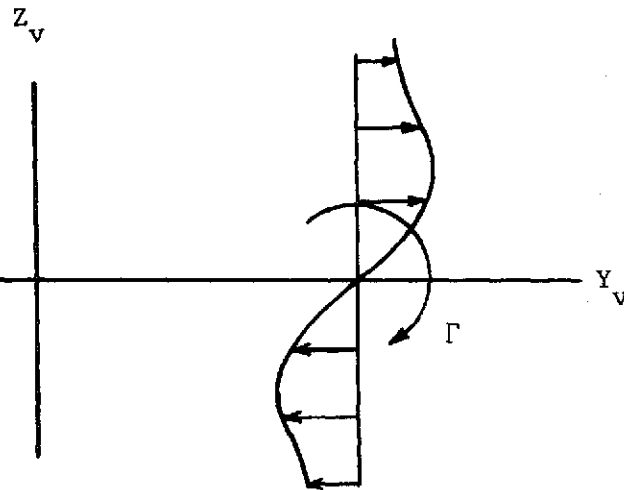


Figure 3. Sketch of Jet Centerline and Vortex Curve with Coordinate Systems

ORIGINAL PAGE IS
OF POOR QUALITY



(a) Typical V_v Distributions Used to Determine Vortex Locations



(b) Typical V_v Distribution Used to Determine Vortex Strength

Figure 4. Typical V_v Distributions in the $Z_v - Y_v$ Plane

ORIGINAL PAGE IS
OF POOR QUALITY

ORIGINAL PAGE IS
OF POOR QUALITY

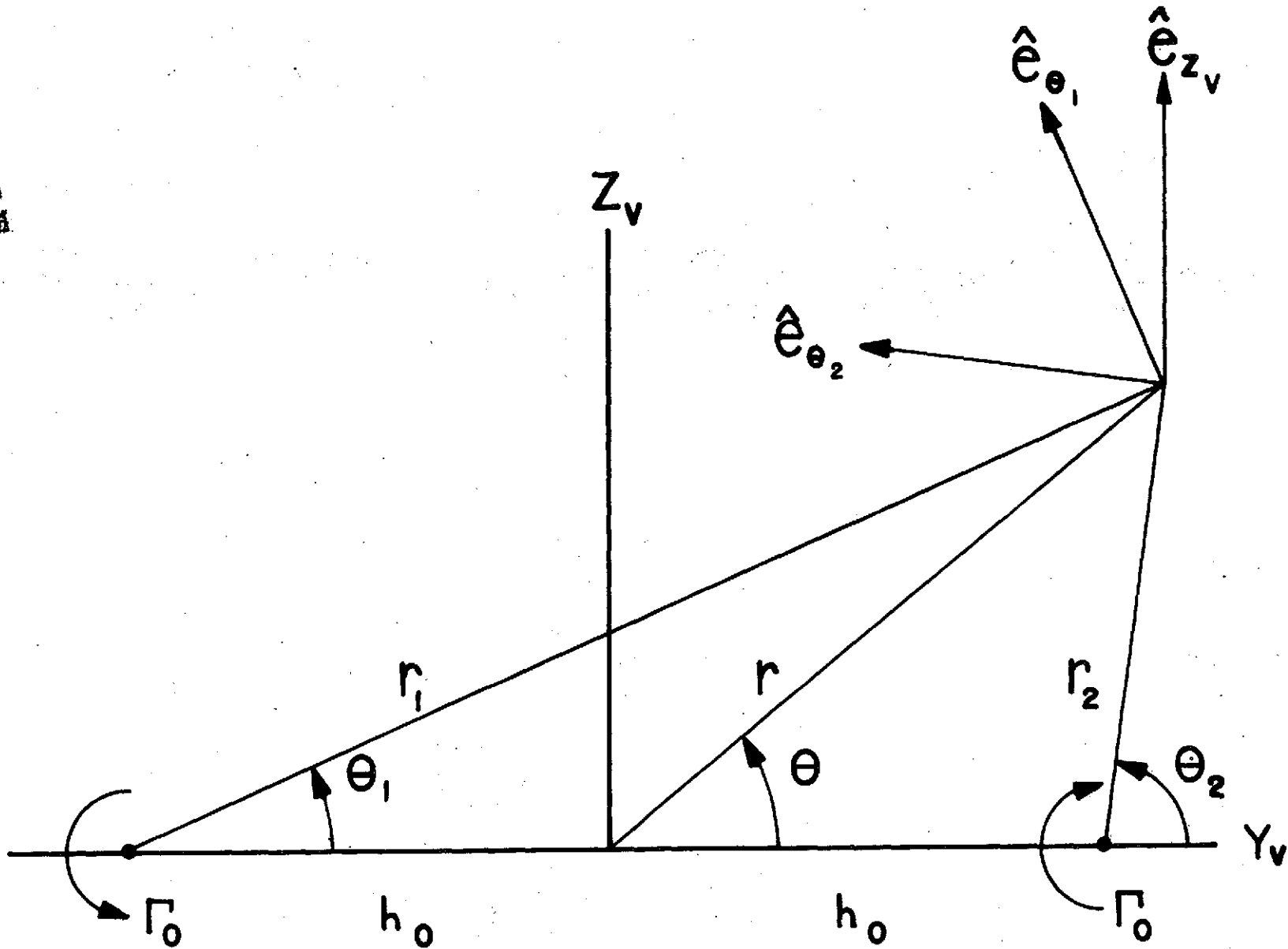


Figure 5. Geometry of Vortex Model

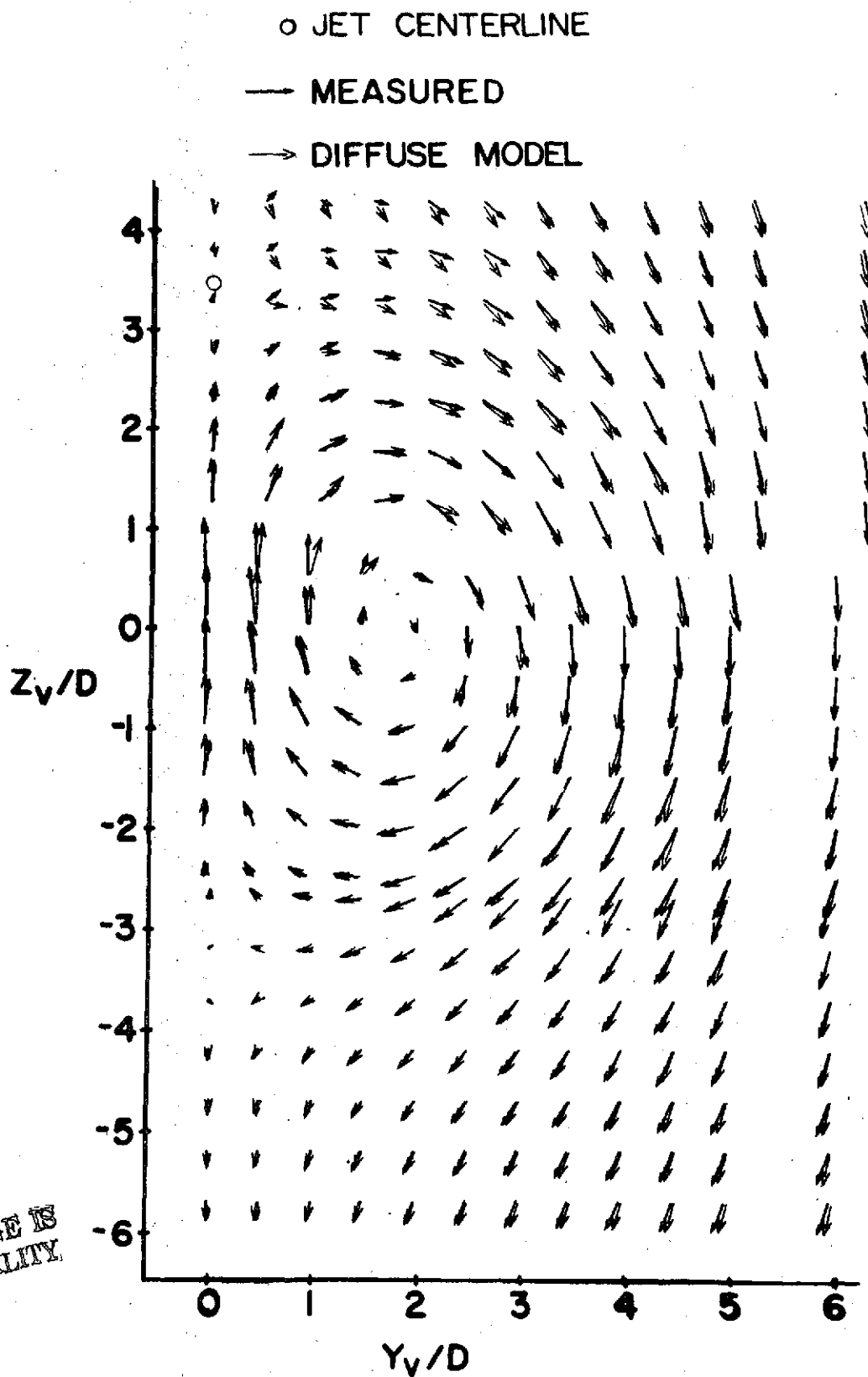


Figure 6. Comparison of Measured and Calculated Velocity Fields for Cross Section at $X/D = 8.3$ and $R = 8$

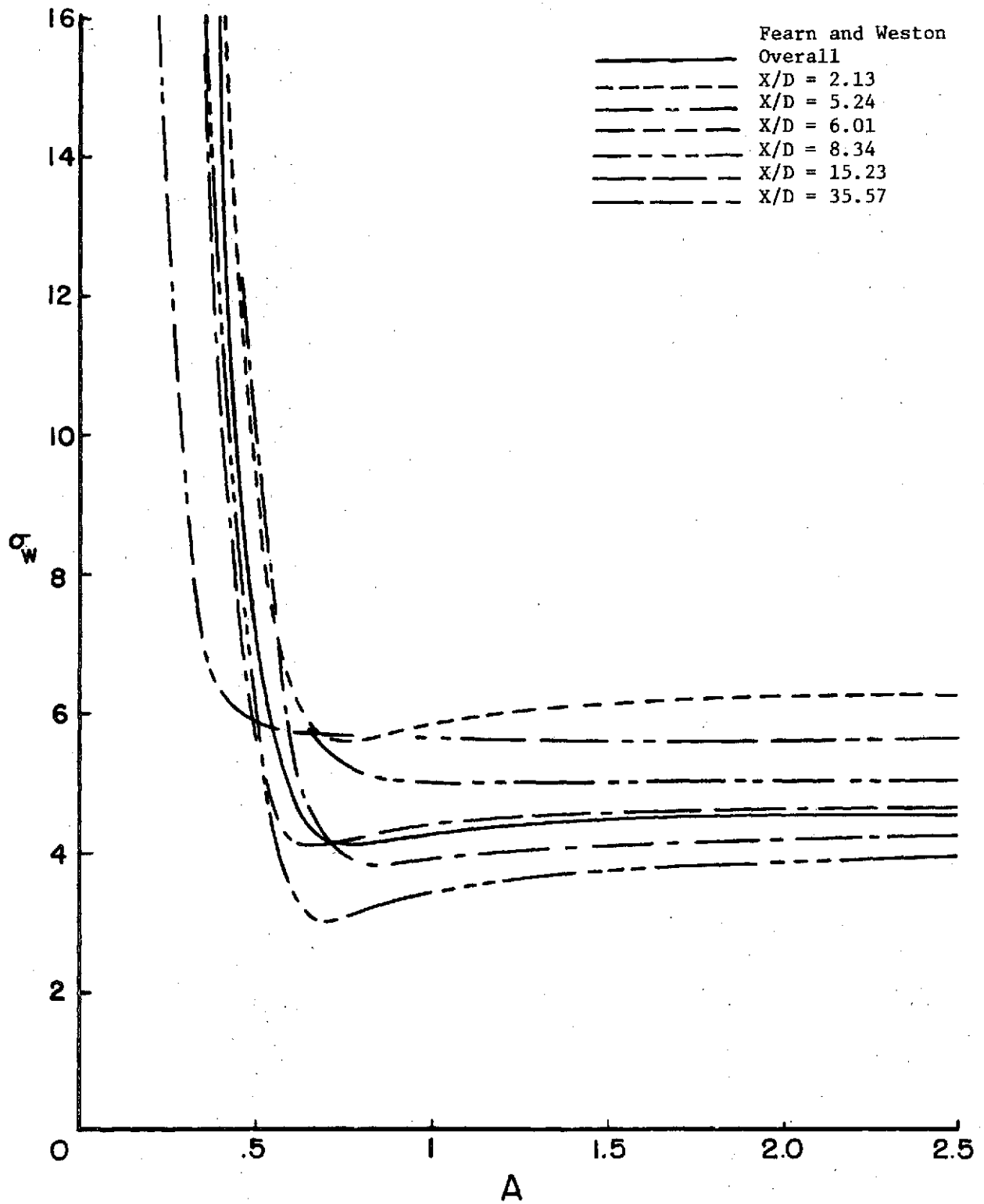


Figure 7. Standard Deviation versus γ_0 , $R = 8$

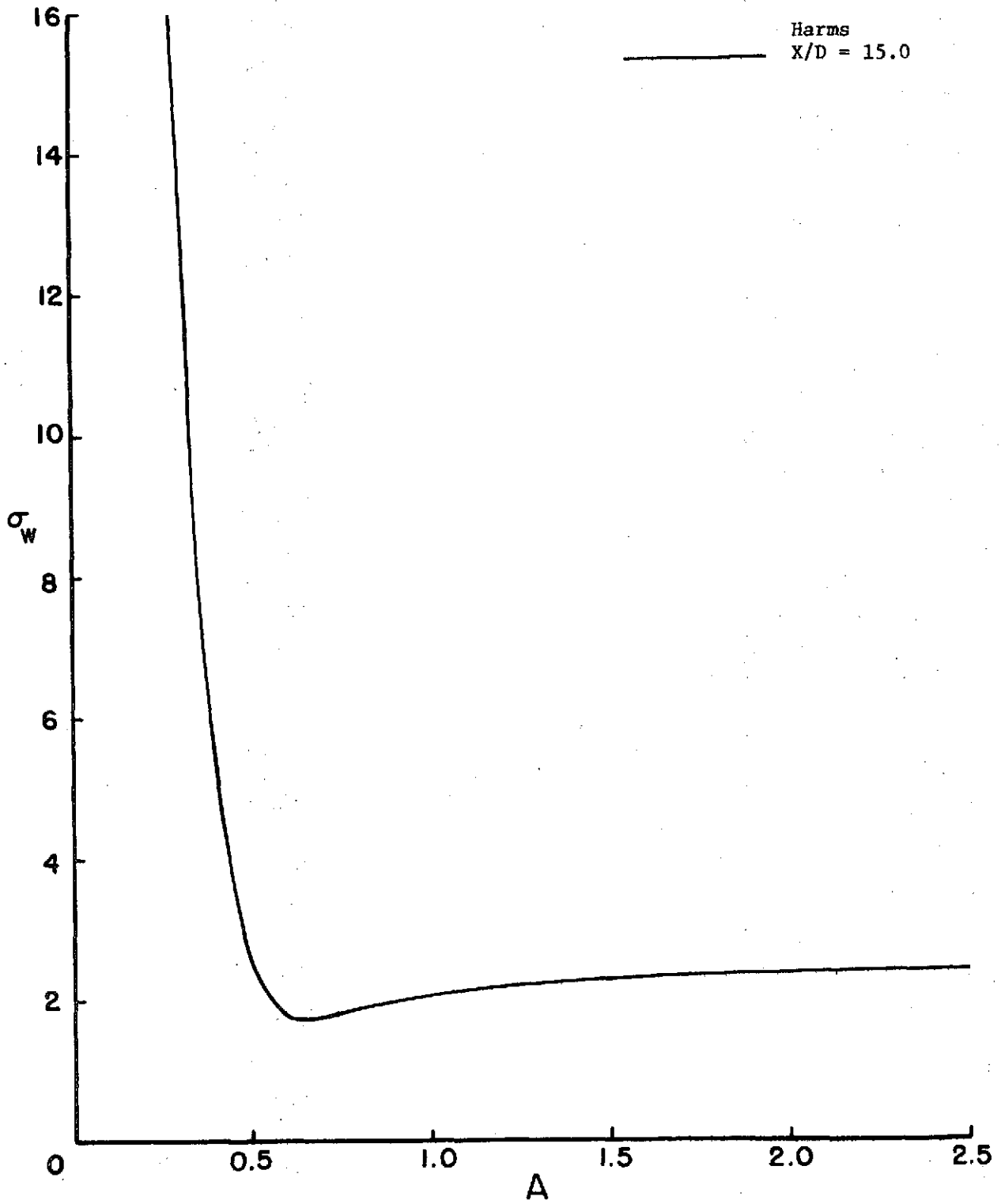


Figure 8. Standard Deviation versus γ_0 , $R=8$

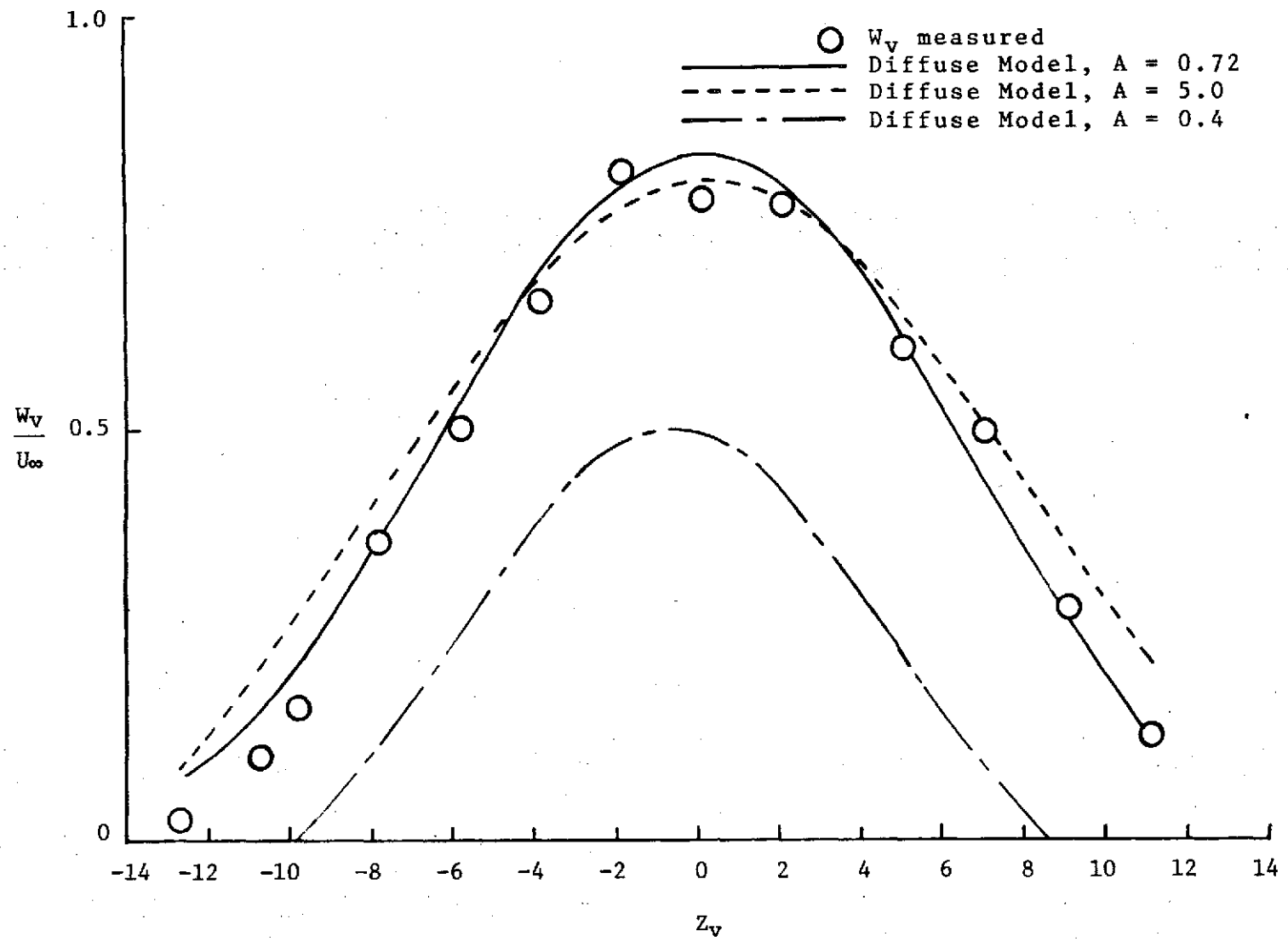


Figure 9. Upwash Velocities along Symmetry Plane
 ($R = 8$, $X/D = 8$, $U_\infty = 127$ ft/sec)

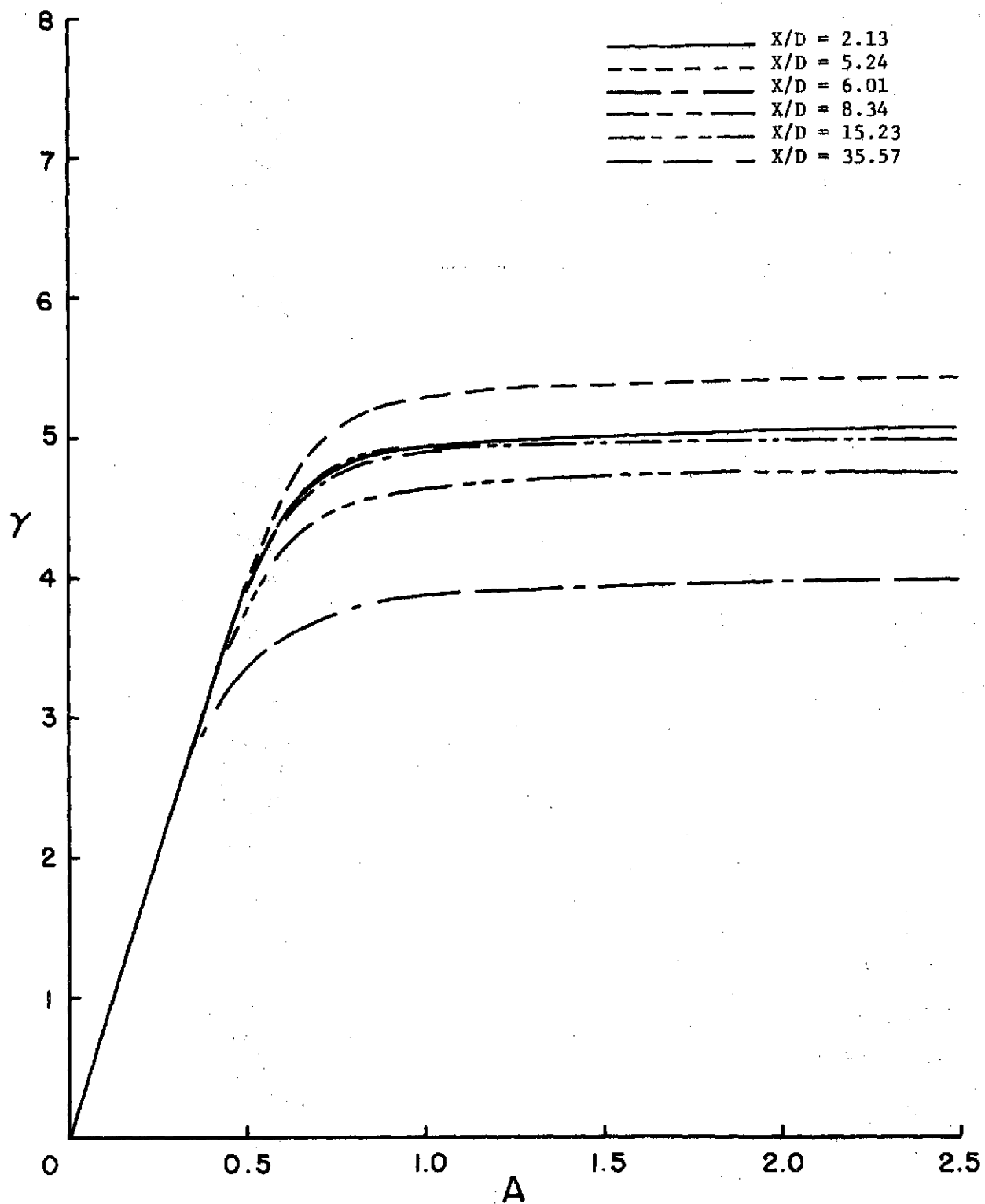


Figure 10. Variation of Vortex Strength with γ_0 , $R = 8$

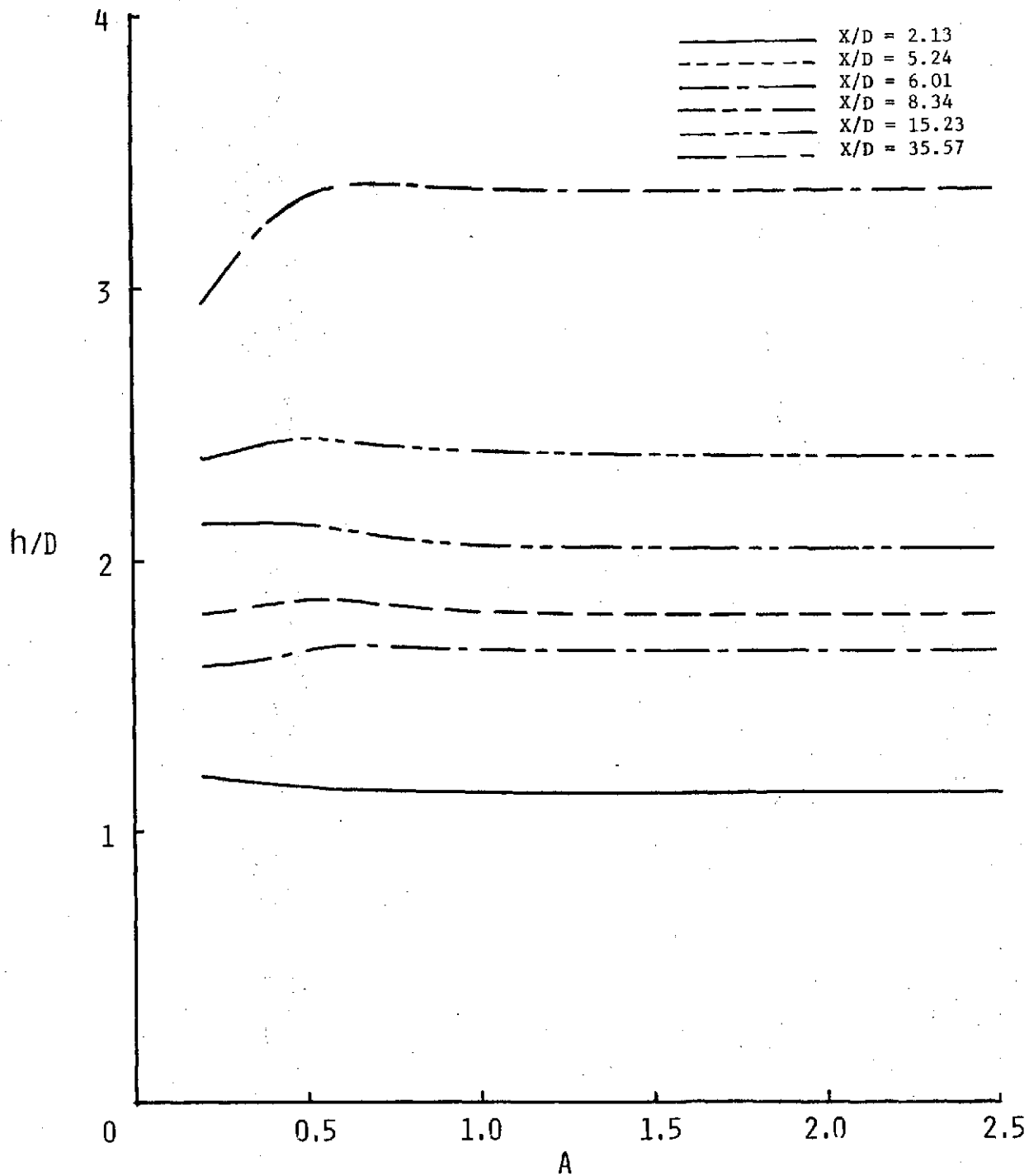


Figure 11. Variation of Effective Vortex Spacing with γ_0 , $R = 8$

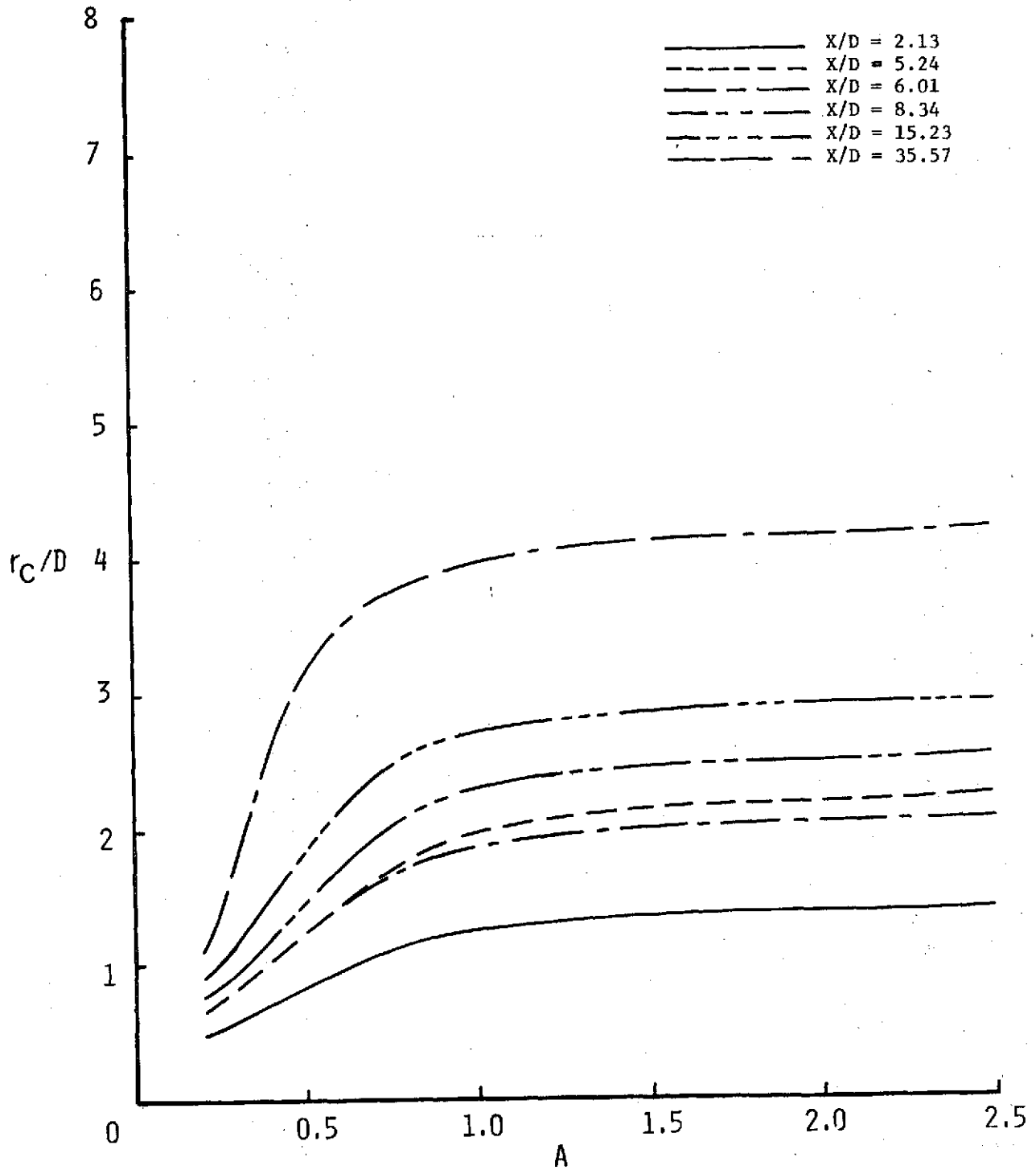


Figure 12. Variation of Vortex Core Size with γ_0 , $R = 8$

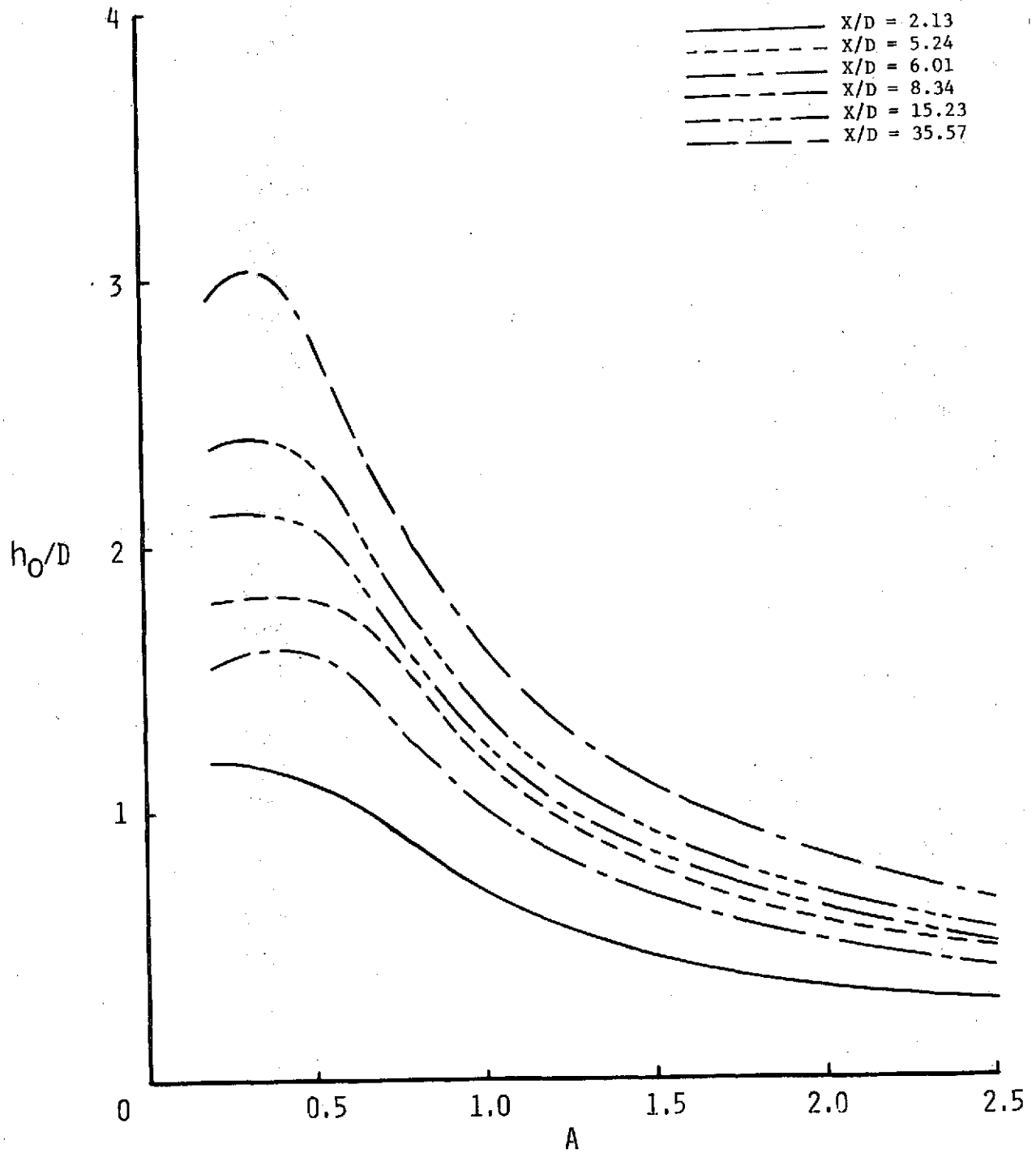


Figure 13. Variation of Vortex Spacing with γ_0 , $R = 8$

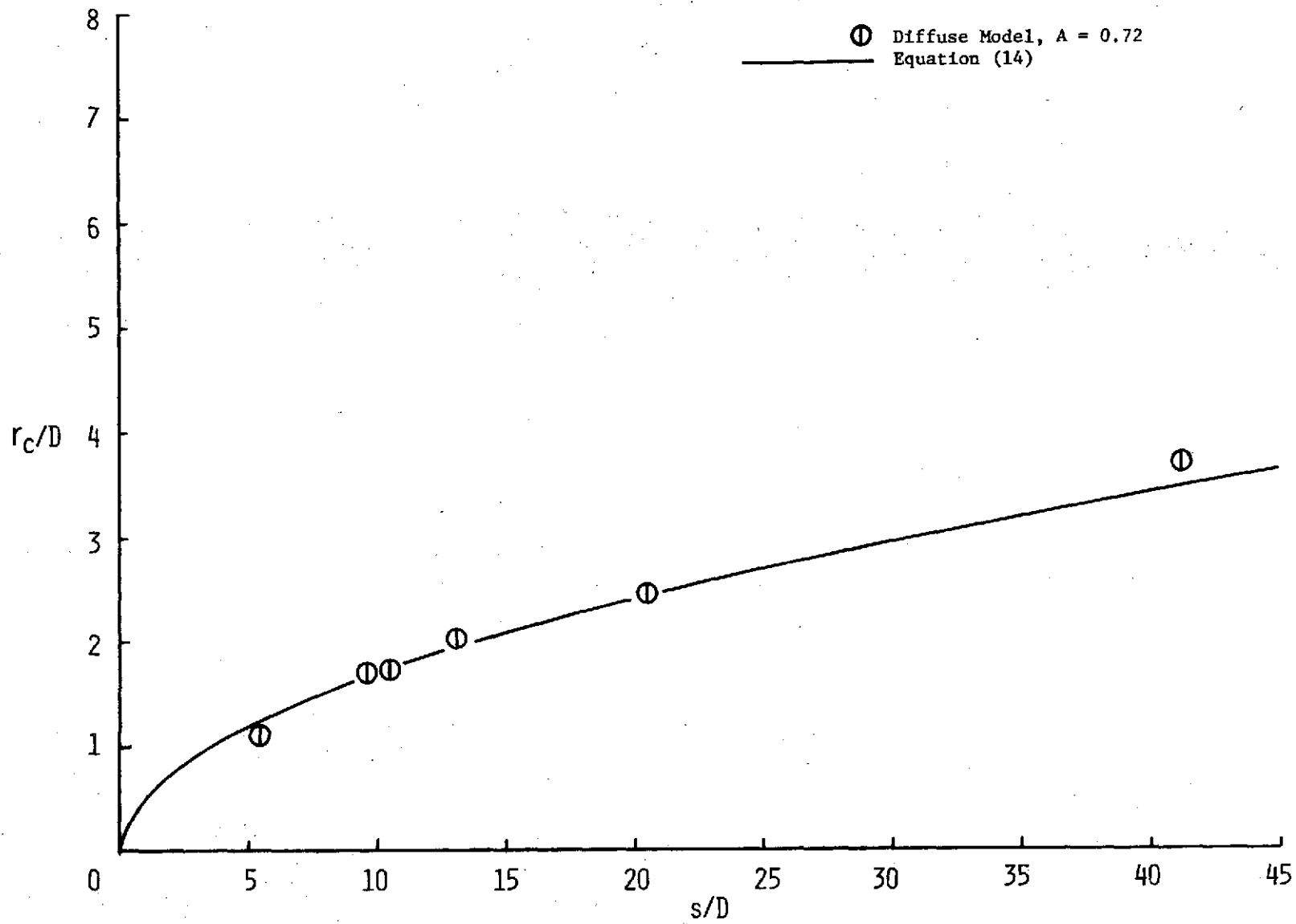


Figure 14. Vortex Core Size, R = 8

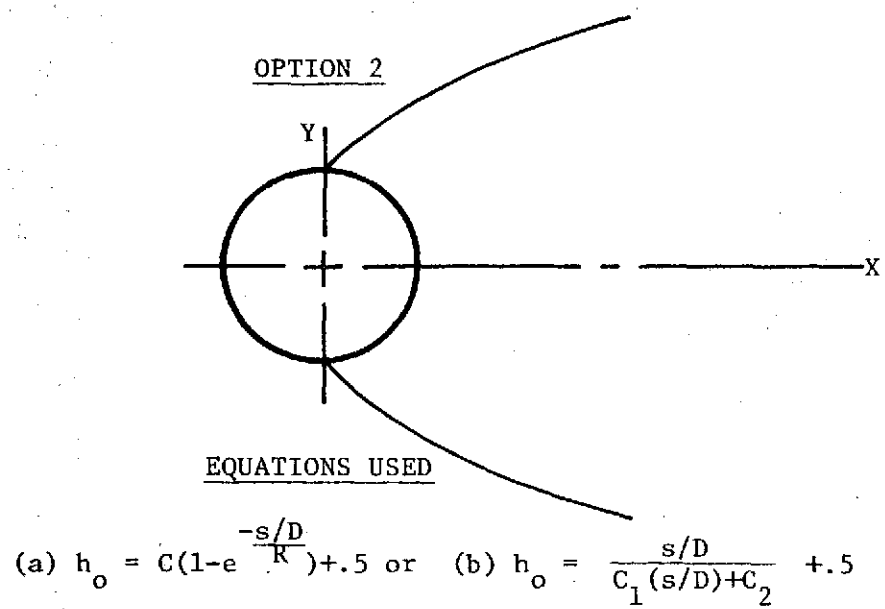
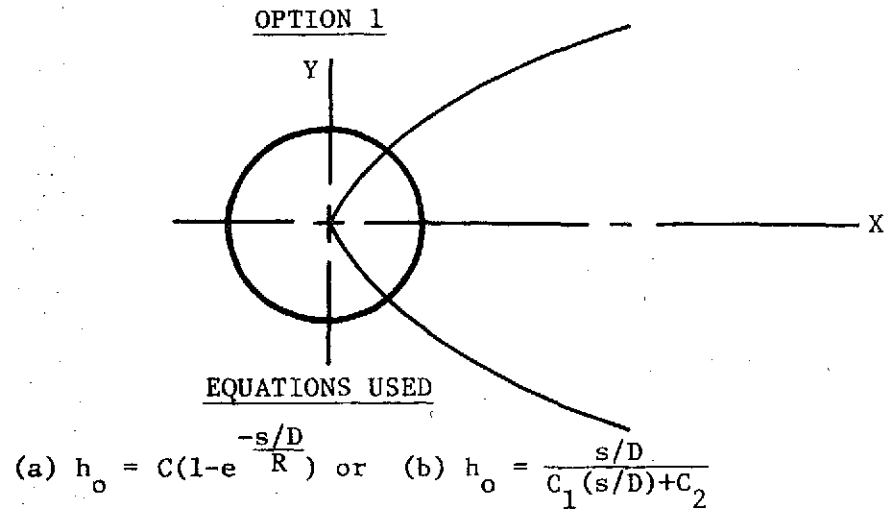
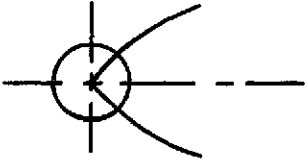
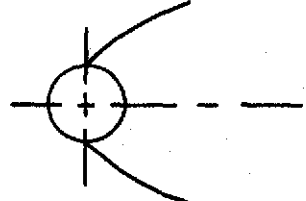


Figure 15. Options for Vortex Spacing

EXTENDED VORTEX MODEL

$$\gamma_o = AR \quad \text{where } A = 0.72$$

$$\beta D = B/(s/D)^{-1/2} \quad \text{where } B = 2.11 \quad (r_c = 1.121/\beta)$$

<p>OPTION (1a)</p> $h_o = C(1 - e^{-\frac{s/D}{R}})$ <p>$C = 2.04$</p>	<p>OPTION (1b)</p> $h_o = \frac{s/D}{C_1(s/D) + C_2}$ <p>$C_1 = 0.425$</p> <p>$C_2 = 2.670$</p>	
<p>OPTION (2a)</p> $h_o = C(1 - e^{-\frac{s/D}{R}}) + 0.5$ <p>$C = 1.389$</p>	<p>OPTION (2b)</p> $h_o = \frac{s/D}{C_1(s/D) + C_2} + 0.5$ <p>$C_1 = 0.504$</p> <p>$C_2 = 5.660$</p>	

$$\gamma = \gamma_o \operatorname{erf}(\beta h_o)$$

$$h = h_o / \operatorname{erf}(\beta h_o)$$

Figure 16. Summary of extended model, $A = 0.72$

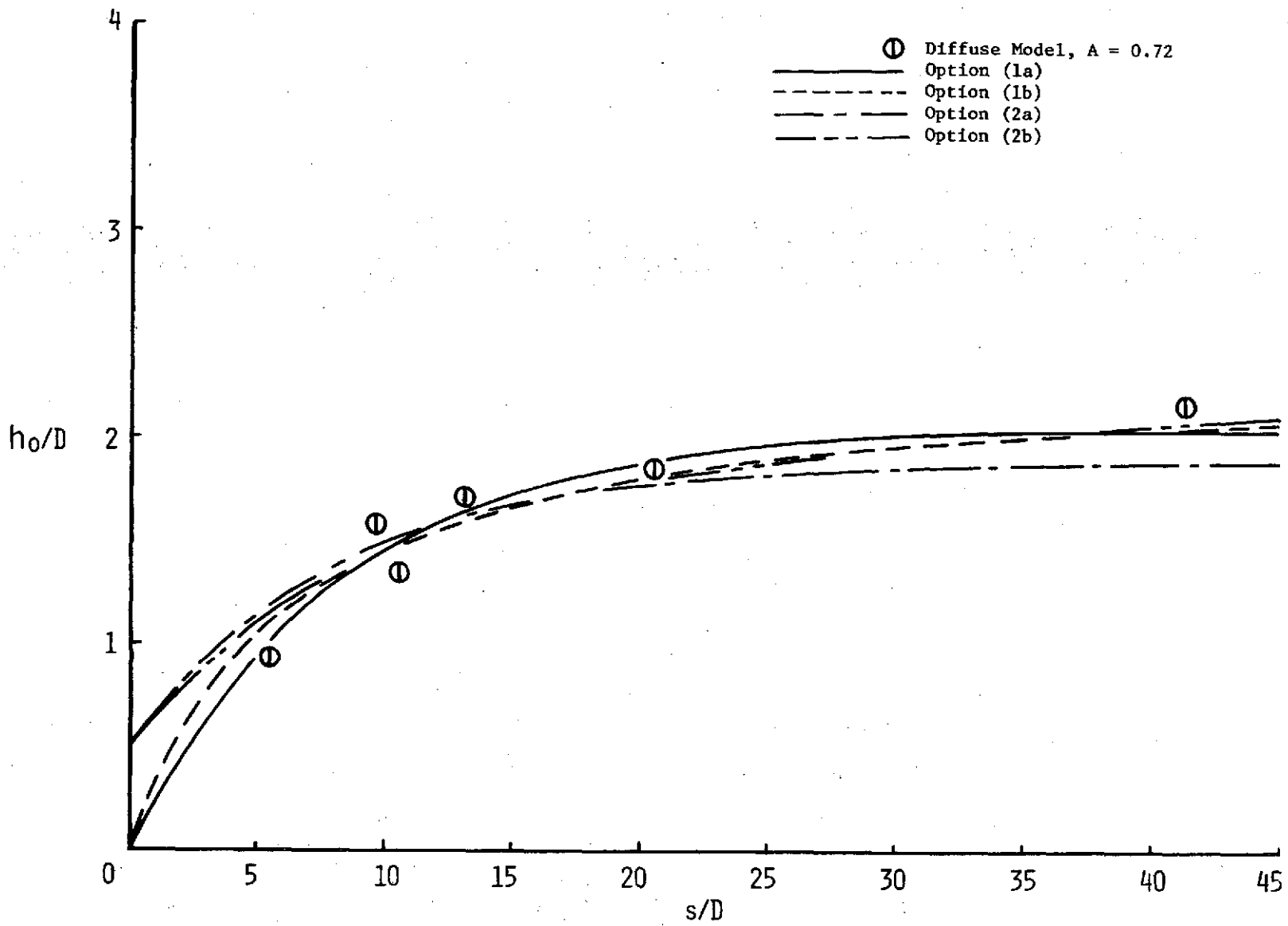


Figure 17. Vortex Spacing, $R = 8$

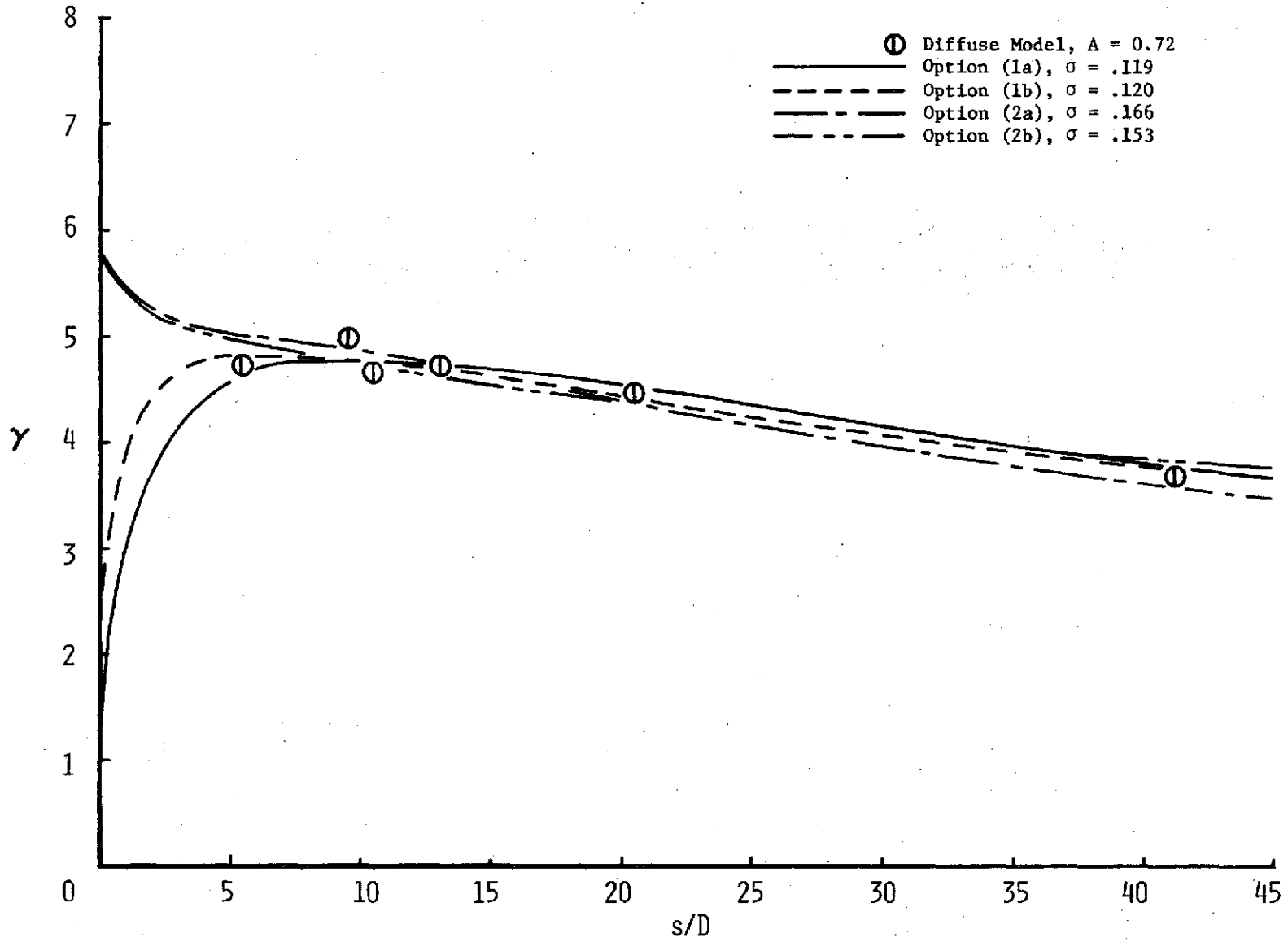


Figure 18. Effective Vortex Strength, $R = 8$

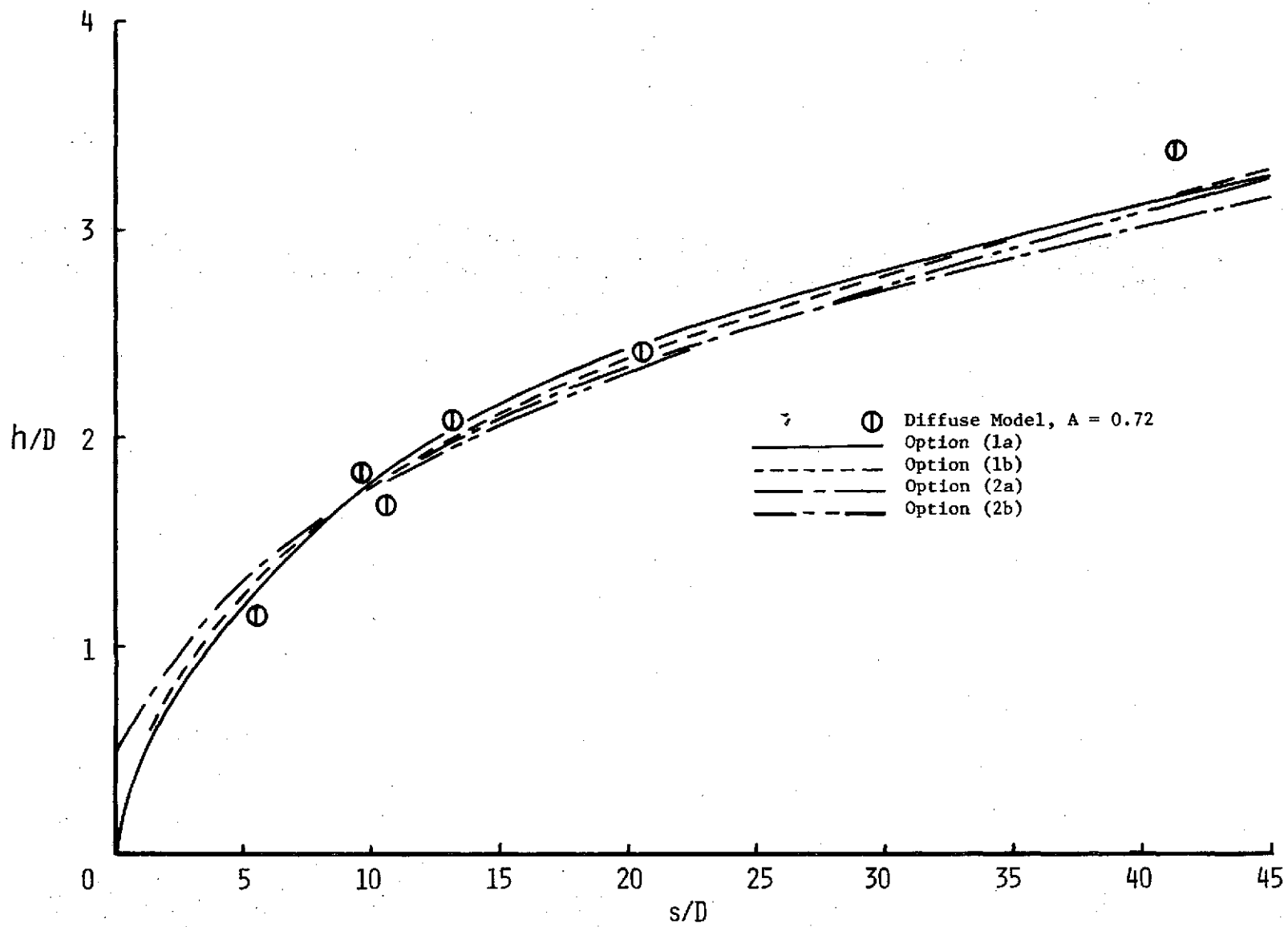


Figure 19. Effective Vortex Spacing, $R = 8$

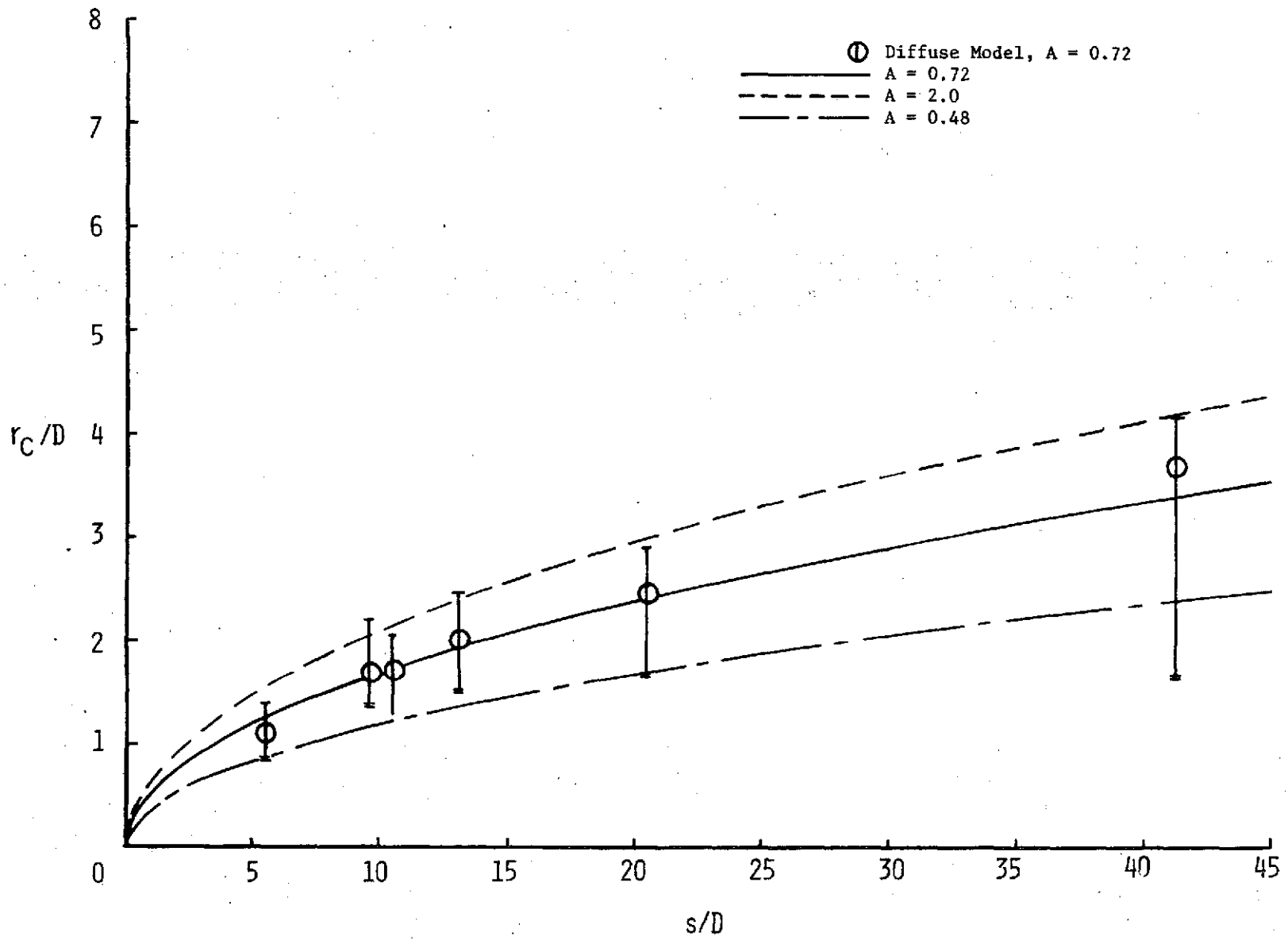


Figure 20. Uncertainty in Vortex Core Size, Equation (14), $R = 8$

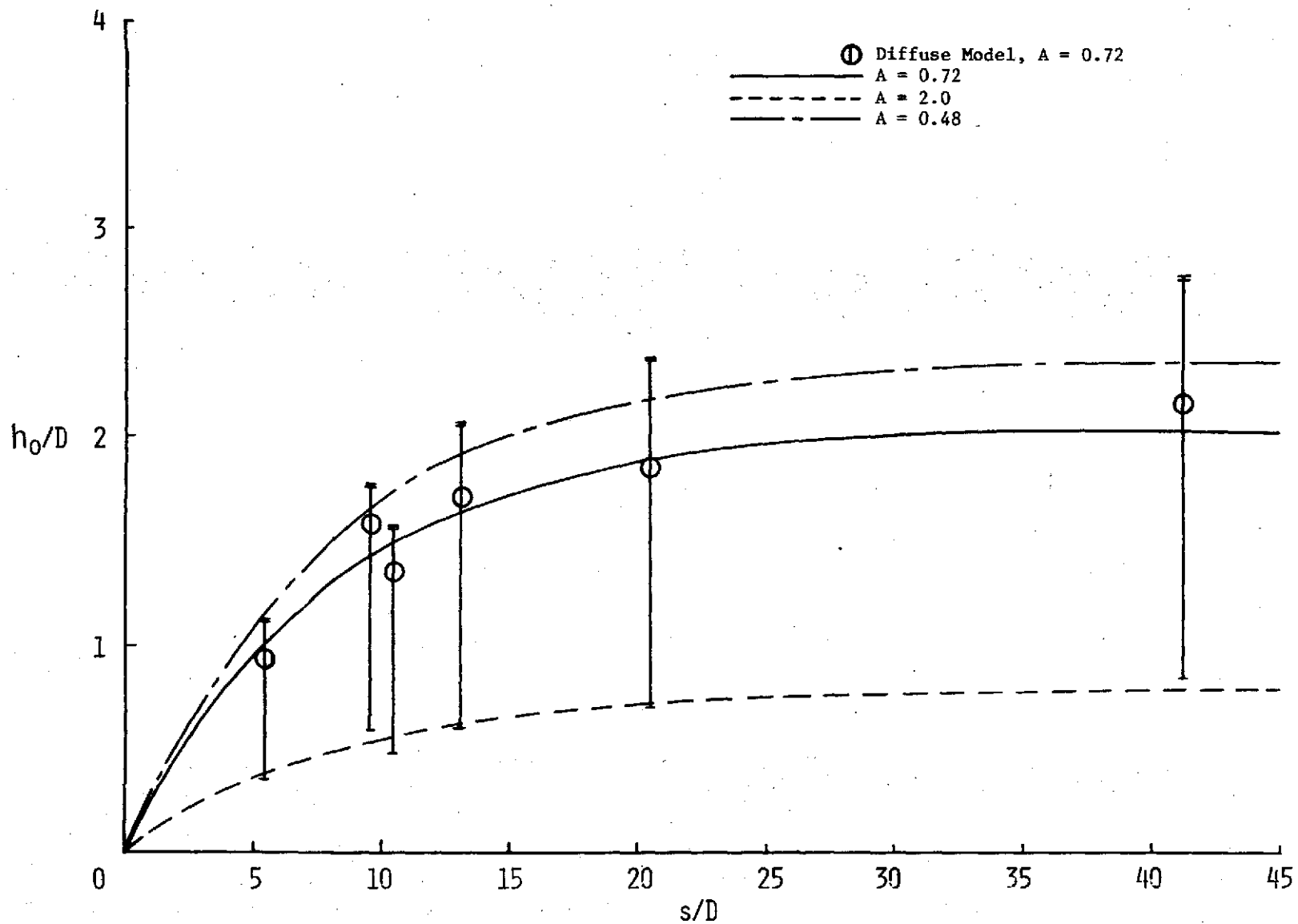


Figure 21. Uncertainty in Vortex Spacing,
Option (1a), $R = 8$

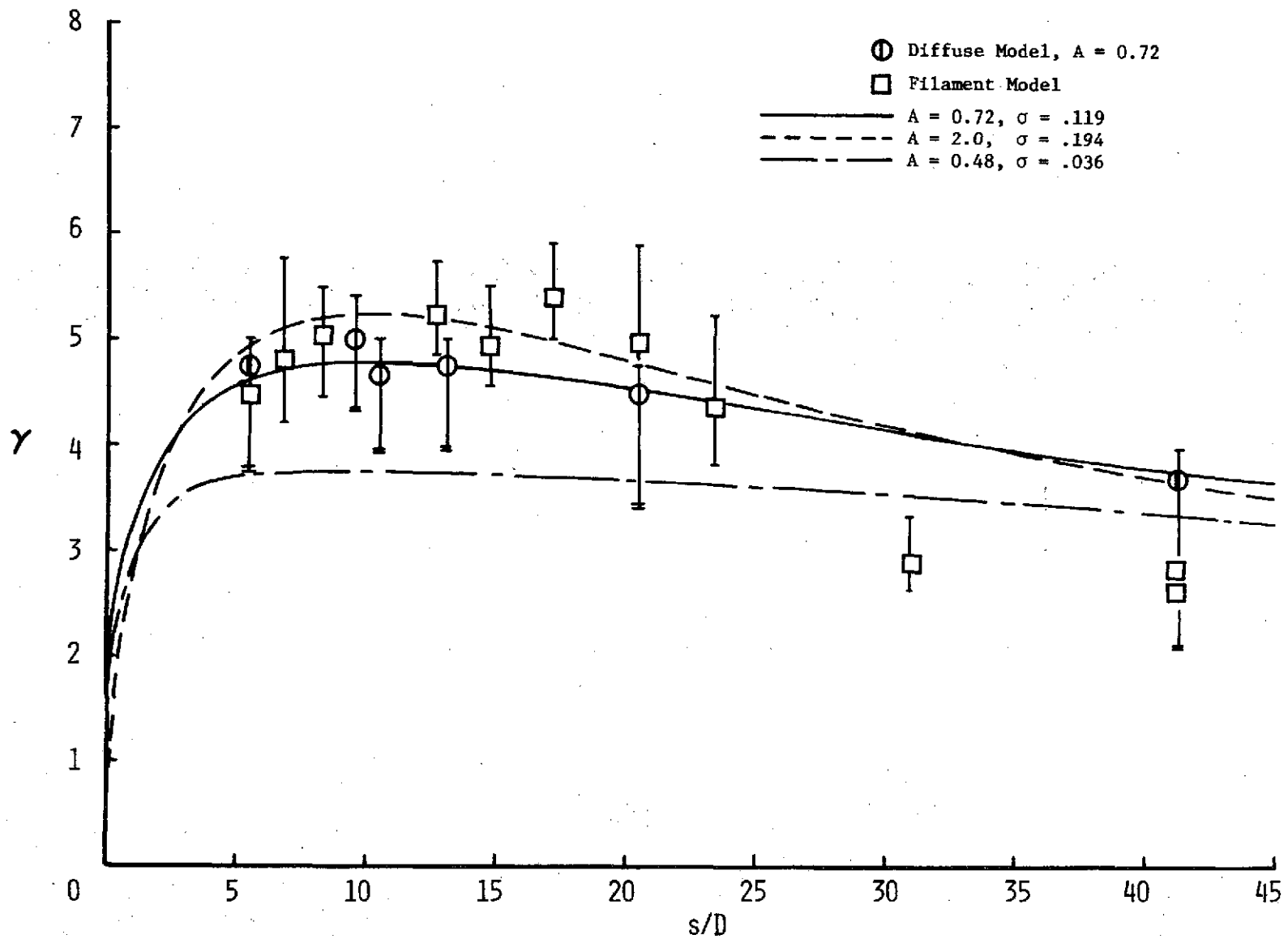


Figure 22. Uncertainty in Effective Vortex Strength, Option (1a), $R = 8$

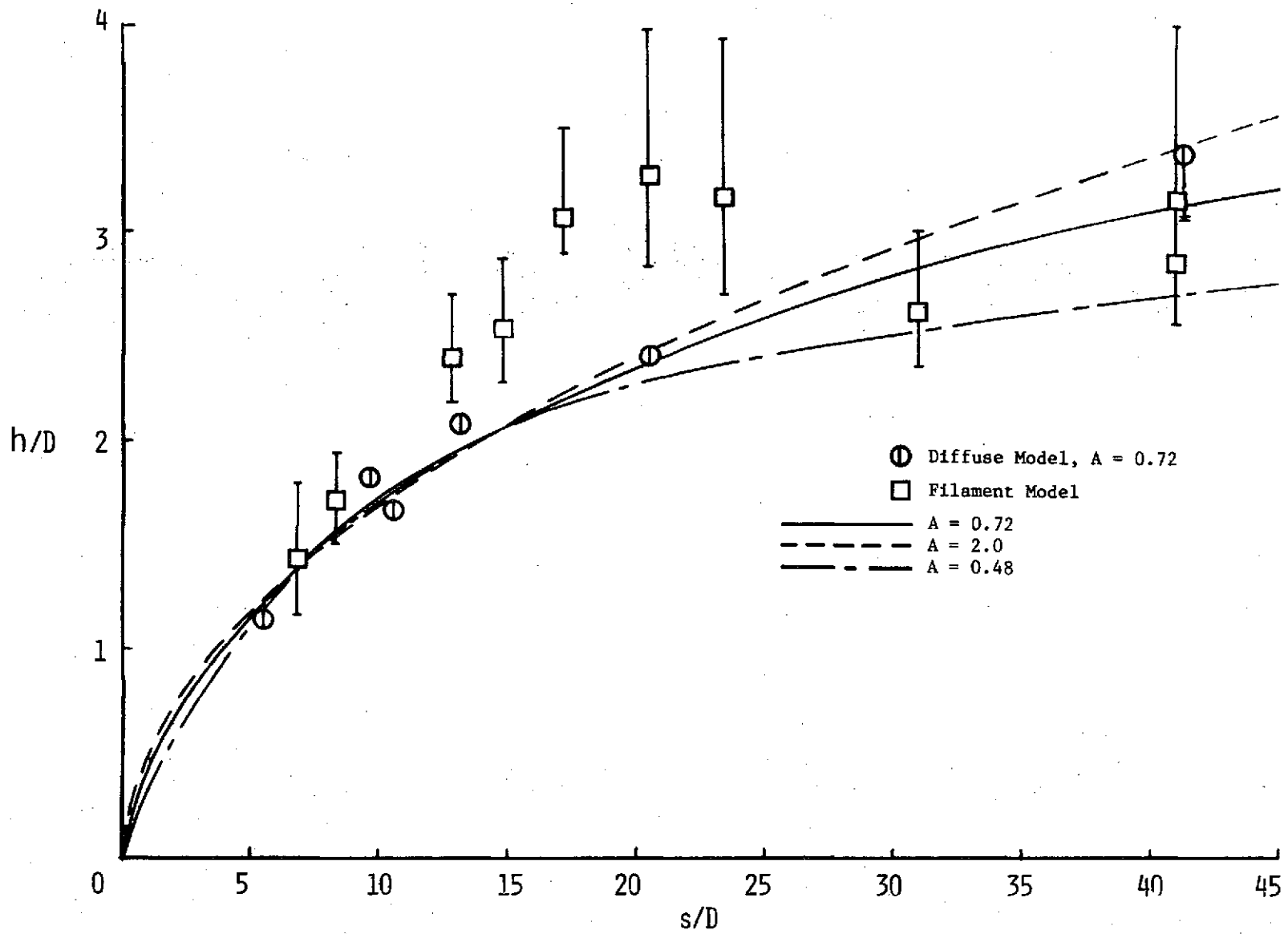


Figure 23. Uncertainty in Effective Vortex Spacing, Option (1a), $R = 8$

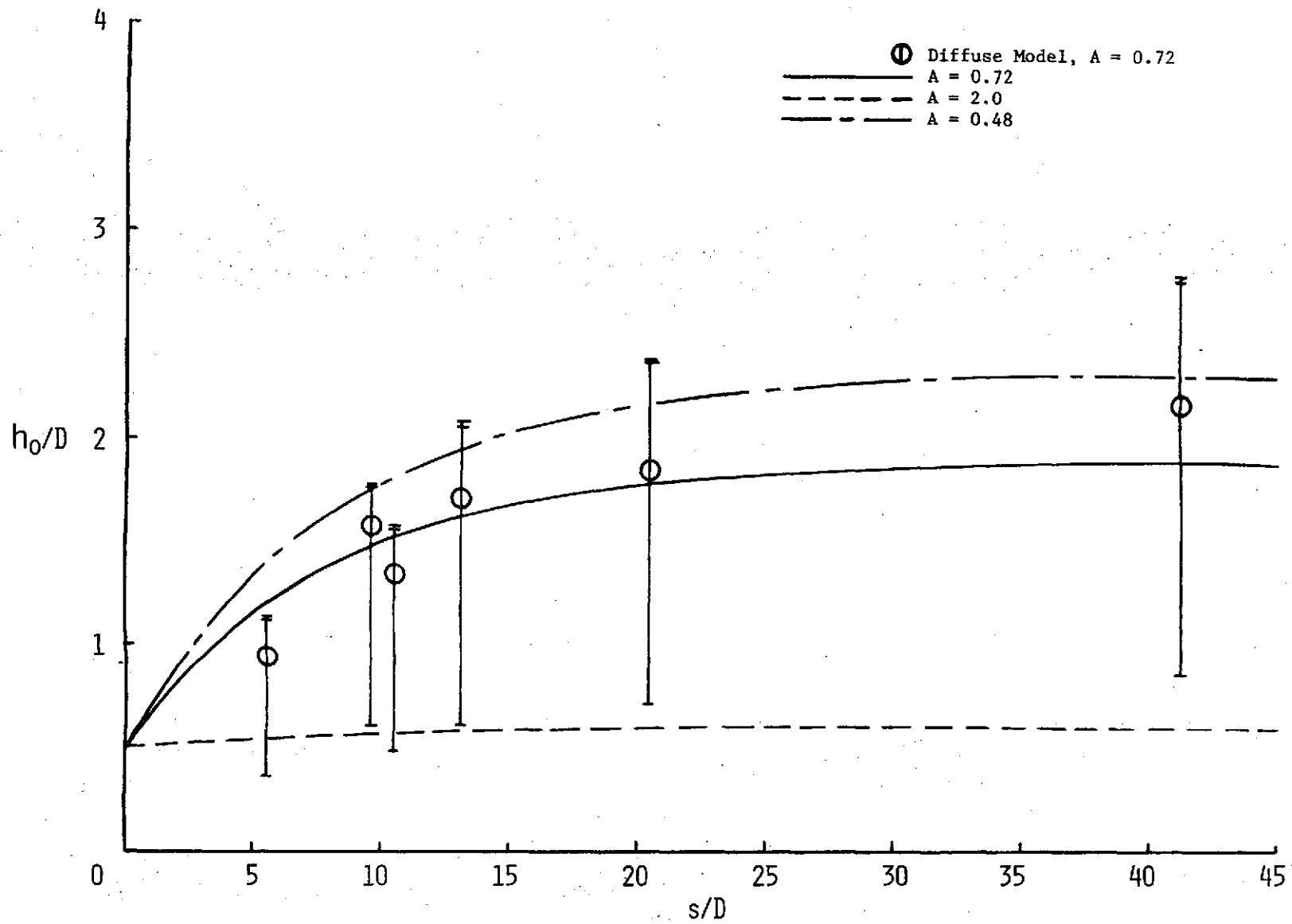


Figure 24. Uncertainty in Vortex Spacing, Option (2a), $R = 8$

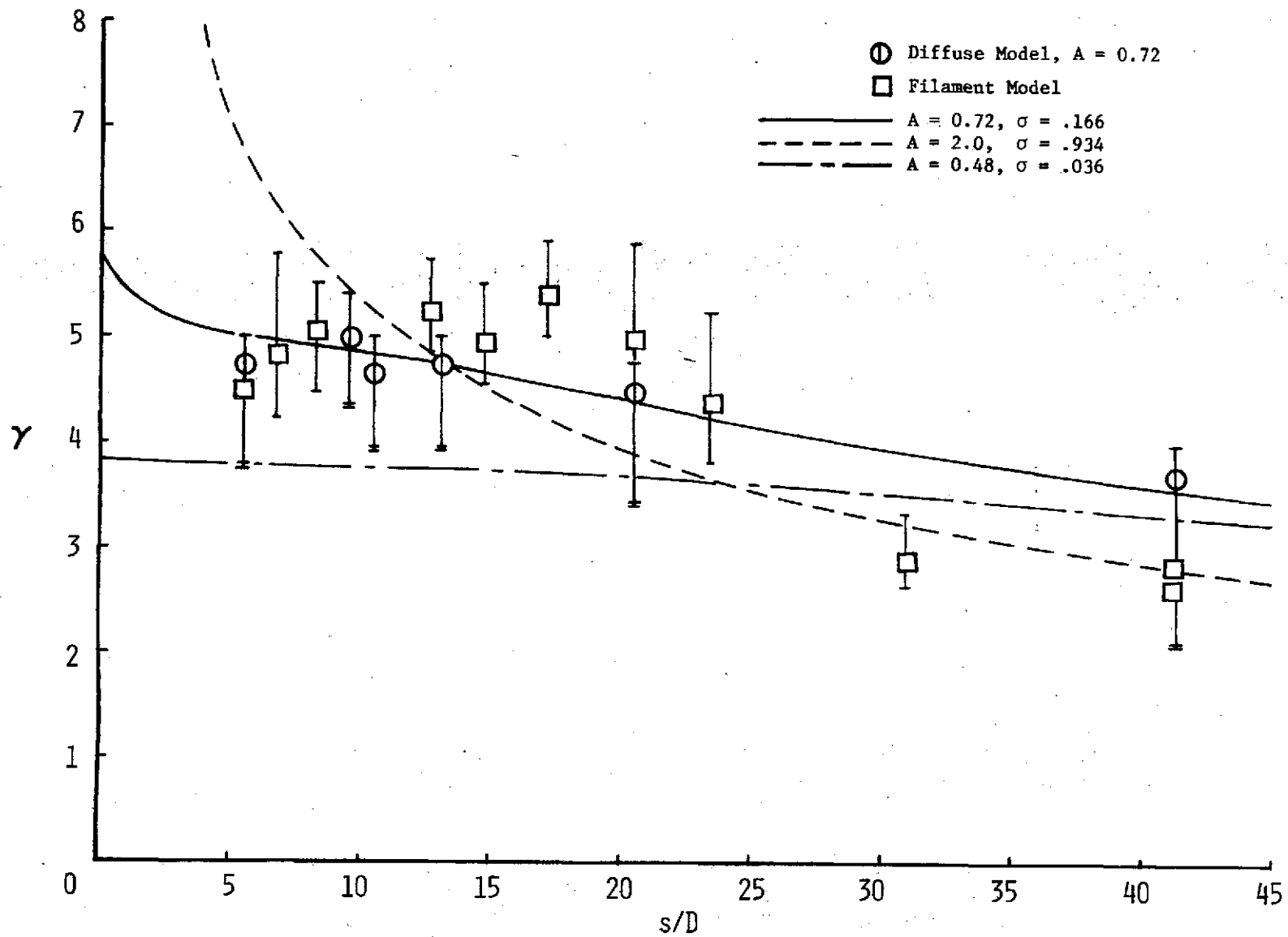


Figure 25. Uncertainty in Effective Vortex Strength, Option (2a), $R = 8$

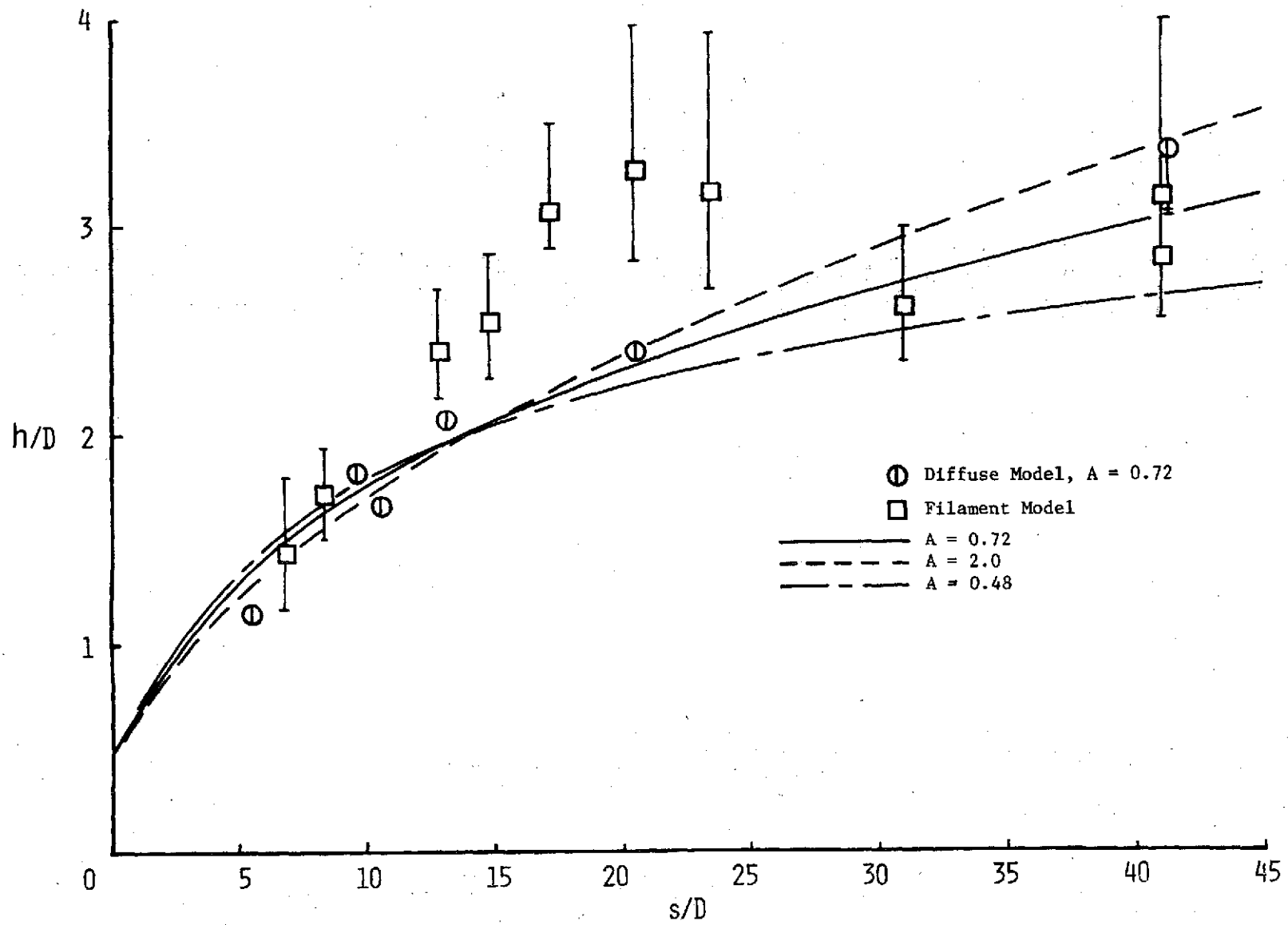


Figure 26. Uncertainty in Effective Vortex Spacing, Option (2a), $R = 8$

TABLE I
SUMMARY OF CROSS SECTION DATA^a, R = 8

VELOCITY MEASUREMENTS	X/D	Z/D	s/D	ϕ_v deg.	CROSS SECTION SIZE	
					JET DIA.	EFF. VORTEX SPACING
49	2.13	4.87	5.52	51.7	2.50D x 2.48D	2.17h x 2.16h
135	5.24	7.56	9.65	33.0	4.99D x 6.97D	2.72h x 3.80h
36	6.01	7.98	10.53	30.7	2.49D x 2.50D	1.48h x 1.49h
216	8.34	9.14	13.11	26.2	6.28D x 8.44D	3.02h x 4.05h
140	15.23	11.83	20.5	18.0	4.49D x 6.52D	1.86h x 2.70h
49	35.57	15.85	41.29	10.9	2.94D x 2.99D	0.87h x 0.89h
b340	15.0	11.16	20.6	17.7	5.41D x 8.43D	2.36h x 3.68h

^a Fearn and Weston (ref. 1)

^b Harms (ref. 3)

APPENDIX I

TWO-PARAMETER DIFFUSE MODEL COMPUTER PROGRAM

```

C THIS PROGRAM FITS A GAUSSIAN-DISTRIBUTED VORTEX PAIR TO THE CROSS-SECTION
C VELOCITY FIELD FOR A JET IN A CROSSFLOW
C ALL VELOCITIES ARE IN FT./SEC.
C A DENOTES THE CIRCULATION IN FT**2/SEC AND GAMMA DENOTES THE DIMENSIONLESS
C CIRCULATION,  $\text{GAMMA} = A / (2 * D * \text{VINFIN})$ , WHERE D IS THE DIAMETER OF THE JET AND
C VINFIN IS THE FREE STREAM VELOCITY.
C B DENOTES THE DIFFUSION CONSTANT IN THE GAUSSIAN DISTRIBUTION. IT HAS UNITS
C OF 1/FT.
C C DENOTES THE HALF SPACING BETWEEN THE CENTERS OF THE TWO DIFFUSE VORTICES.
C H DENOTES THE HALF SPACING IN JET DIAMETERS,  $H = C / D$ . LET BETA DENOTE THE
C DIMENSIONLESS DIFFUSION CONSTANT,  $\text{BETA} = B * C$ .
C DIMENSION RMSG(6),RMST(6),P(6),S(3),MBC(5)
C COMMON IYZCOD, IYZ, NR, NC, A, B, C, ZC, VINFIN, VSINA, VY(21,12), VZ(21,12),
C IY(3,12), Z(21), RMS, NDRPF, IPRNT, NPTS, IRMS, RMSVZO(2,5), IPRTM, NRAK
C COMMON/ONE/MK, NCATA, IRUN(4), R, AMJET, X4, Z4, SD, ANGVRT, VRANG
C REAL*8 P, S, D
C DO 2 I=1,6
C 2 RMST(I)=0.0
C CTR=1.745329E-2
C READ 1, CCNST, GPER, IPRTM, IRMS
C 1 FORMAT(14X, F8.3, 17X, F8.6, 7X, I1, 6X, I1)
C IF IPRTM=0 ,NO MATRICES PRINT OUT. IF IPRTM=1 ,ALL MATRICES PRINT OUT.
C IF IPRTM=2 ,VORTICITY MATRIX DOESNT PRINT OUT, BUT OTHERS DO.
C IF IRMS=0, OVERALL FIT IS IN PER CENT IF IRMS=1 OVERALL FIT IS IN FT/SEC
C GPER=.01*GPER
C DO 10 I=1,6
C 10 RMSG(I)=0.0
C NG=0
C NBC=0
C 20 N=0
C VINFIN=0.
C AMJET=0.
C CONSULT FORMAT NO. 50 FOR DESCRIPTION OF VARIABLES IN FOLLOWING STATEMENT
C READ(5,30,END=9999) ANGVRT, ZC, NRAK, NDRPF, NDRPL, NC, GAMMA, BETA, H, NZ,

```



```

      1ZOC
C   NZ IS THE NUMBER OF THE RAKE CONTAINING THE VORTEX CENTER.
C   ZOC=STEP CHANGE IN Z USED IN ZC PERTURBATION ANALYSIS
      30 FORMAT(10X,F4.1,8X,F5.2,5X,I1,12X,I1,17X,I1/I2,37X,3(F5.2,6X),I1;
      1F7.2)
C   A1 AND D1 USED IN REFERENCING RAKE POSITIONS IN THE CROSS-SECTION
      40 A1=TAN(ANGVRT*CTR)
      C1=SQRT(1.+A1*A1)
C   NR=NO. OF ROWS OF DATA
      NR=7*NRAK-NDRPF-NDRPL
      IZ=7
      IF(NZ.EQ.NRAK) IZ=7-NDRPL
      WRITE(6,50) ANGVRT,ZO,IZ,NZ,ZOC,NRAK,NDRPF,NDRPL,NC,GAMMA,BETA,H
      50 FORMAT('1INPUT DATA  VORTEX ANGLE =',F5.1,' DEG',7X,'ZO =',F6.2,
      1' IN. FROM PROBE',I2,' OF RAKE',I2,7X,'DELTA ZO =',F5.2/
      1      15X,I1,' RAKES OF INPUT ',I2,' PROBES FROM FIRST RAKE ARE D
      2ELETED'/33X,I1,' PROBES FROM LAST RAKE ARE DELETED'/15X,I2,' YAW
      3POSITIONS'/' INITIAL ESTIMATESO  GAMMA =',F5.2/ 21X,' BETA  =',
      4F5.2/ 21X,' H      =',F5.2)
      R=0.
C   DC LOOP 110 READS IN VELOCITY FIELD DATA AND RAKE POSITIONS, AND CONVERTS
C   THESE TO THE CROSS-SECTION COORDINATE SYSTEM
      DC 110 I=1,NRAK
      READ(5,60) IRUN(I),ANGRAK,Q,RHO,X4,Z4,A2,(Y(I,J),J=1,NC)
      60 FORMAT(3X,I3,11X,F4.1,3X,F6.3,5X,F8.6,2(4X,F5.2),3X,F5.2/12F6.2)
      R=R+A2
      IF(I.EQ.1) C1=Z4-A1*X4
      D4=(A1*X4-Z4+C1)/D1
      VINI=VINI+SQRT(2.*Q/RHO)
      DA=(ANGRAK-ANGVRT)*CTR
      SINDA=SIN(DA)
      COSDA=COS(DA)
      LI=I
      L=L+1

```

```

M=L
IF(I.EQ.1) L1=1+NDRPF
IF(I.EQ.1) L=L1
N=N+7
IF(I.EQ.NRAK) N=N-NDRPL
IF(I.NE.NZ) GO TO 70
XD=X4/4.
ZD=Z4/4.
RAKEZC=ZC
VRCCS=COSDA
VRANG=ANGRAK*DTR
IZ=N
ZO=ZC*COSDA
ZOC=ZOC*COSDA/12.
70  DO 90 K=1,NC
    READ(5,80) (VY(J,K),VZ(J,K),Z(J),J=M,N)
80  FORMAT(11F7.2/10F7.2)
    IF(I.EQ.NRAK .AND. NDRPL.GT.3) READ(5,80) DA
    DO 90 J=L,N
        VY(J-L1+1,K)=VY(J,K)
90  VZ(J-L1+1,K)=Z(J)*SINDA + VZ(J,K)*COSDA
    DO 100 J=L,N
100 Z(J-L1+1)=D4+(J-L+L1)*2.*COSDA
110 IF(I.EQ.1) N=N-NDRPF
    R=R/NRAK
    GAMMA=CONST*R
    IF(NZ.EQ.1) IZ=IZ-NDRPF
    VINFINF=VINFINF/NRAK
C  COMPUTE NOMINAL JET MACH NUMBER USING ESTIMATE OF PINF (2130. PSFA)
    AMJET=R*SQRT(Q/(C.7*2130.))
    NOMR=INT(R+0.5)
    CALL QMAJ(NOMR,A1,A2,A3)
    MK=0
    IF(ABS(Q-A3).LT.2.) MK=3

```

ORIGINAL PAGE IS
OF POOR QUALITY

```
IF (ABS(Q-A2) .LT. 2.) MK=2
IF (ABS(Q-A1) .LT. 2.) MK=1
VSINA=VINP*SIN(ANGVRT*DTR)
CG 120 J=1,NR
120 Z(J)=Z(NR)-Z(J)
Z0=Z(IZ)+Z0
REFZ0=Z0
C DETERMINE INITIAL ESTIMATES
A=2.*VINP*GAMMA/3.
C=H/3.
B=BETA/C
BSAV=B
CSAV=C
WRITE(6,130) A,B,C,VINP,R,(IRUN(I),I=1,NRAK)
130 FORMAT(/14H A(FT**2/SEC)=,F10.2,' B(1/FT)=,F10.4,' C(FT)=,F10.3/
1' AVG VINP =,F6.1/' AVG R =,F6.2/' RUNS READ INO,4I4)
PRINT 135,AMJET,MK
135 FORMAT(/' NOMINAL MACH NO. =,F5.3,10X,' Q CONDITION =,I2)
A1=VRANG/DTR
PRINT 140,NZ,XD,ZD,A1
140 FORMAT(/' PROBE 4 OF RAKE',I2,' AT X/D =,F6.2,' Z/D =,F6.2,2X,
1' RAKE ANGLE =,F5.1,' DEG')
CALL AUXIL
C SET Z SPACING OF 5 VORTEX CENTER CASES. FOR PERTURBATION ANALYSIS.
RMSVZO(2,1)=0.
RMSVZO(2,2)=-24.*ZOC
RMSVZO(2,3)=-ZOC*12.
RMSVZO(2,4)=ZOC*12.
RMSVZO(2,5)=24.*ZOC
ZOSAVZ=Z0
RMS=0.
MG=-1
C MG IS THE INDEX OF THE GAMMA0 AND VELOCITY COMPONENT BEING CONDUCTED.
IGF=C
```

```
      CC 720 KG=1,3
C   DC ANALYSIS FOR 3 SETTINGS OF GAMMAO
      IF(KG.EQ.2) A=(1.+GPER)*A
      IF(KG.EQ.3) A=(1.-GPER)*A/(1.+GPER)
      ZOSAV=ZOSAVZ
C   DC ANALYSIS FOR FIT TO Z VELOCITY COMPONENT.
      JLZ=1
C   IF LAST TIME BOMBED OUT, RESET INITIAL GUESSES. OTHERWISE, START WITH
C   RESULTS OF PREVIOUS TIME.
      IF(RMS.EQ.0.) GO TO 340
      BSAVZ=B
      CSAVZ=C
      GC TC 350
340  BSAVZ=BSAV
      CSAVZ=CSAV
350  ZO=ZOSAV
      IYZ=3-JLZ
      IYZCCD=IYZ
C   IYZCODE=1 FOR VY CALCULATION   =2 FOR VZ CALCULATION
      NIT=0
C   NIT IS NUMBER OF RE-SHIFTS OF ZO. LIMITED TO 9.
      IF(KG.EQ.1) WRITE(6,360)
360  FORMAT(1F1)
370  NIT=NIT+1
      ZOP=ZO*12.
      IF(KG.EQ.1) PRINT 380,NIT,ZOP
380  FORMAT(/' ITER =',I2,' , ZO =',F6.2)
      IPRNT=0
      IRC=C
      IF(NIT.EQ.9) GO TO 540
C   DC LCCP 430 PERFORMS FIT FOR 5 ZO CASES
      CC 430 LZ=1,5
      IF(LZ.EQ.1) GO TO 390
      IF(LZ.EQ.2) ZO=ZO-2.*ZOC
```

```
IF(LZ.EQ.3) Z0=ZC+ZOC
IF(LZ.EQ.4) Z0=ZC+2.*ZOC
IF(LZ.EQ.5) Z0=ZC+ZOC
390 IF(JLZ.EQ.1 .AND. KG.NE.1) GO TO 400
IF(RMS.EQ.0.) GO TO 410
BSAV=B
CSAV=C
GO TO 420
400 BSAV=BSAVZ
CSAV=CSAVZ
410 B=BSAV
C=CSAV
420 CALL DIFCOR
C DIFCOR CALCULATES LEAST SQUARE FIT TO THE VELOCITIES
RMSVZO(1,LZ)=RMS
IF(RMS.EQ.0.) IRC=IRO+1
C IRC IS THE NUMBER OF BOMB-CUTS OF THE 5 ATTEMPTS.
430 CONTINUE
Z0=ZC-2.*ZOC
IF(IRO.GT.2) GO TO 470
IF(KG.EQ.1) PRINT 440,((RMSVZO(I,J),I=1,2),J=1,5)
440 FORMAT(' RMS =',F8.4,' AT VZC =',F6.2)
P(1)=0.0
P(2)=0.0
P(3)=0.0
P(4)=0.0
P(5)=0.0
S(1)=0.0
S(2)=0.0
S(3)=0.0
C PERFORM SUMMATIONS FOR PARABOLIC FIT TO RMS VERSUS Z0
DO 460 I=1,5
IF(RMSVZO(1,I).EQ.0.) GO TO 460
A1=1.
```

```

CC 450 J=1,5
P(J)=P(J)+A1
IF(J.GT.3) GC TO 450
S(J)=S(J)+A1*RMSVZO(1,I)
450 A1=A1*RMSVZO(2,I)
460 CONTINUE
CALL MINV3(P,D)
IF(D.NE.0.) GC TO 560
470 PRINT 480,((RMSVZO(I,J),I=1,2),J=1,5)
480 FORMAT(/' NO PARABOLIC SOLUTION TO RMS VERSUS Z0'/' INPUT WASO'/
1(' RMS =',F8.4,' AT VZO =',F6.2))
IF(NIT.EQ.9) GO TO 530
IF(IRC.NE.5) GO TO 510
IPRNT=3
C IF ALL 5 ATTEMPTS FAILED, LCOP 500 SEARCHES FOR A SOLUTION BY VARYING Z0 UP
C AND DOWN.
CC 500 J=1,6
IF(J.EQ.1) Z0=Z0-3.*Z0C
IF(J.EQ.2) Z0=Z0-Z0C
IF(J.EQ.3) Z0=Z0-Z0C
IF(J.EQ.4) Z0=Z0+8.*Z0C
IF(J.GE.5) Z0=Z0+Z0C
B=BSAV
C=CSAV
CALL DIFCOR
ZOP=Z0*12.
PRINT 490,RMS,ZOP
490 FORMAT(' RMS=',F8.4,' AT Z0=',F6.2)
IF(RMS.NE.0.) GC TO 370
500 CONTINUE
GO TO 530
C520 AN ATTEMPT THAT WORKED IS USED AS THE NEW CENTER OF THE Z0 SPREAD.
510 CC 520 J=2,5
IF(RMSVZO(1,J).EQ.0.) GC TO 520

```

ORIGINAL PAGE IS
OF POOR QUALITY

```
IF(J.EQ.2) Z0=ZC-2.*ZOC
IF(J.EQ.3) ZC=ZC-ZOC
IF(J.EQ.4) ZC=ZC+ZOC
IF(J.EQ.5) ZC=ZC+2.*ZOC
GO TO 370
520 CONTINUE
530 *G=MG+2
    IF(JLZ.EG.1) ICF=1
    GO TO 720
540 PRINT 550
550 FORMAT(/' ITERATION LIMIT EXCEEDED IN FITTING RMS VERSUS Z0')
    GO TO 470
C COMPUTE NEW Z0 (AT MINIMUM OF THE LSQ PARABOLIC FIT)
560 DZ0=(S(1)*P(2)+S(2)*P(4)+S(3)*P(5))/(24.*(S(1)*P(3)+S(2)*P(5)+
    1S(3)*P(6)))
    A1=5.*ZOC
    IF(ABS(DZ0).GT.A1) DZ0=SIGN(A1,DZ0)
    Z0=Z0-DZ0
C METHOD IS ITERATED UNTIL THE ZC VERSUS RMS CURVE HAS ITS MINIMUM WITHIN THE
C Z0 RANGE.
    IF(ABS(DZ0).GT.(1.2*ZOC)) GO TO 370
    ZOP=Z0*12.
    PRINT 570,ZOP
570 FORMAT(/' FINAL VALUE FOR ZC =',F7.2)
    A1=.25*(RAKEZO+(ZOP-REFZC)/VRCOS-6.)
    X4=XC-A1*SIN(VRANG)
    Z4=ZC+A1*COS(VRANG)
    A1=Z4-.347308*R**1.126536*X4**.429137
    SD=ARCLNG(X4,R) + A1*SIN(ANGVRT*DTR)
    PRINT 580,X4,Z4,SD
580 FORMAT(/' VORTEX CENTER AT X/D =',F6.2,'', Z/D =',F6.2,10X,'ARC LEN
    1GTH (S/D) =',F6.2)
    IPRNT=1
C NOW PERFORM LEAST SQUARES FIT AT THE MINIMUM RMS LOCATION.
```

```

590 CALL DIFCOR
      IF (KG.NE.1) GO TO 710
      IF(IPRTM.EQ.0) GO TO 710
      CALL PRMAT
                                                    $$$$$$$$
710 NG=NG+2
C   PERFORM SUMMATIONS FOR OVERALL RMS COMPUTATIONS FOR ALL CASES AT THE SINGLE
C   VELOCITY RATIO BEING CONSIDERED.
      RMST(MG)=RMS*RMS*NDATA
      IF(JLZ.EQ.2) GO TO 720
      ZOSAVZ=ZC
      IF(RMS.EQ.0.) ZCSAVZ=ZCSAV
720 CONTINUE
      IF(IGF.NE.1) GO TO 730
C   IGF=1 IF ONE OF THE GAMMA CASES BOMBED OUT IN FITTING Z COMPONENT.
C   THIS RUN IS THEN NOT INCLUDED IN THE OVERALL RMS CALCULATION.
      NBC=NBC+1
      MBC(MBC)=IRUN(1)
      GO TO 20
730 DO 740 I=1,6
740  RMSG(I)=RMSG(I)+RMST(I)
      NG=NG+NDATA
      GO TO 20
9999 DO 10000 I=1,6
10000 RMSG(I)=SQRT(RMSG(I)/NG)
      A1=(1.+GPER)*CCNST
      A2=(1.-GPER)*CONST
      PRINT 10010,RMSG(1),RMSG(2), CONST ,RMSG(3),RMSG(4),A1,RMSG(5),
1      IRMSG(6),A2
10010 FORMAT(///1X,28(1H*)/29H *RMS VALUES FOR OVERALL FIT*/1X,28(1H*)//
1' Z RMS =',F8.4,', Y RMS =',F8.4,' FOR CENTRAL CCNST =',F6.3/
2' Z RMS =',F8.4,', Y RMS =',F8.4,' FOR HIGH CONST =',F6.3/
3' Z RMS =',F8.4,', Y RMS =',F8.4,' FOR LOW CONST =',F6.3)
      A1=GPER*CCNST
      A2=(RMSG(3)-RMSG(5))/(2.*A1)

```



```

A3=(RMSG(3)+RMSG(5)-2.*RMSG(1))/(2.*A1*A1)
A1=-0.5*A2/A3
B=CCNST+A1
A=RMSG(1)+A1*(A2+A3*A1)
IF(IRMS.EQ.0) PRINT 10020,A,B,NG
10020 FORMAT(/' MINIMUM RMS =',F8.4,' PER CENT AT CONST =',F6.3//15,' PO
INTS OF DATA')
IF(IRMS.EQ.1) PRINT 10021,A,B,NG
10021 FORMAT(/' MINIMUM RMS =',F8.4,' FT/SEC AT CONST =',F6.3//15,' PCIN
ITS OF DATA')
IF(NBC.EQ.0) STCP
PRINT 10030,(MBC(I),I=1,NBC)
10030 FORMAT(/' RUNS NOT USED',5(I4,' ', '))
STCP
END
SUBROUTINE DIFCCR
C THIS SUBROUTINE PERFORMS LEAST SQUARE FITTING USING THE DIFFERENTIAL
C CORRECTION METHOD FOR A GAUSSIAN-DISTRIBUTED VORTEX PAIR.
C TWO PARAMETER FIT TO GAMMA IS HELD CONSTANT B AND C ARE VARIED FOR BEST FIT.
COMMON IYZCOD,IYZ,NR,NC,A,B,C,ZO,VINF,VSINA,VY(21,12),VZ(21,12),
IY(3,12),Z(21),RMS,NCRPF,IPRNT,NPTS,IRMS,RMSVZO(2,5),IPRTM,NRAK
COMMON/DNE/MK,NCATA,IRUN(4),R,AMJET,X4,Z4,SC,ANGVRT,VRANG
COMMON/DVD/FIB,FIC
DATA ERRCR/4.0E-4/
C ERRCR = ACCEPTABLE ERROR FOR VARIABLE COEFFICIENTS.
IF(IPRNT.EQ.2) GO TO 100
ITER=0
IYZCOD=IYZ
C TWO VARIABLE COEFFICIENTS ( B,C )
C
C PERFORM SUMMATIONS FOR COEFFICIENTS IN NORMAL EQUATIONS
10 SFB2=0.0
SFC2=C.0
SFBC=0.0

```

ORIGINAL PAGE IS
OF POOR QUALITY

```
SFBR=0.0
SFCR=0.0
SRI2=0.0
NPTS=C
DO 20 I=1,NR
K=(I+NDRPF+6)/7
DO 20 J=1,NC
IF(VY(I,J).GT.500.) GO TO 20
IF(IYZ.EQ.1) VZY=VY(I,J)
IF(IYZ.EQ.2) VZY=VZ(I,J)+VSINA
RI=F(Y(K,J),Z(I))-VZY
FIA=DF(Y(K,J),Z(I))
SRI2=(SRI2+RI*RI)
SFB2=SFB2 + FIB*FIB
SFC2=SFC2 + FIC*FIC
SFBC=SFBC + FIB*FIC
SFBR=SFBR - FIB*RI
SFCR=SFCR - FIC*RI
NPTS=NPTS+1
20 CONTINUE
RMS=SQRT(SRI2/NPTS)
C SOLVE NORMAL EQUATIONS FOR THE CORRECTIONS TO THE ESTIMATES
D =SFB2*SFC2 - SFBC*SFBC
IF(D.EQ.0.) GO TO 999
B1=(SFBR*SFC2 - SFCR*SFBC)/D
C1=(SFB2*SFCR - SFBC*SFBR)/D
IF(ITER.GT.20) GO TO 40
IF(ITER.GT.10) GO TO 70
IF(ABS(B1/B).GT..05) GO TO 30
IF(ABS(C1/C).LT..05) GO TO 70
C DAMP THE CORRECTIONS
30 IF(ITER.GT.5) GO TO 50
FRAC=(ITER+3)/20.
GO TO 60
```

ORIGINAL PAGE IS
OF POOR QUALITY

```
40 FRAC=0.5
   GO TO 60
50 FRAC=(ITER-1)/10.
60 B1=FRAC*B1
   C1=FRAC*C1
C  UPDATE ESTIMATES AND TEST FOR CONVERGENCE
70 ITER=ITER+1
   B=B+B1
   C=C+C1
   IF(IPRNT.EQ.3) PRINT 80,ITER,RMS,A,B,C
80 FORMAT(20X,'ITER=',I3,' ',RMS=',F8.4',' ',A=',F8.4',' ',B=',F8.4',' ',C=',
  1,F8.4)
   IF(ITER.GT.30) GO TO 999
   IF(B.LT.C.) B=-B
   IF(ABS(B1/B).GT.ERROR.OR.ABS(C1/C).GT.ERROR) GO TO 10
   SRI2=0.
C  COMPUTE STANDARD DEVIATIONS.
   DO 90 I=1,NR
   K=(I+NDRPF+6)/7
   DO 90 J=1,NC
   IF(VY(I,J).GT.500.) GO TO 90
   IF(IYZ.EQ.1) VZY=VY(I,J)
   IF(IYZ.EQ.2) VZY=VZ(I,J)+VSINA
   RI=F(Y(K,J),Z(I))-VZY
   SRI2=(SRI2+RI*RI)
90 CONTINUE
   RMS=SQRT(SRI2/NPTS)
   IF(IRMS.EQ.1) GO TO 95
   IF(IPRNT.EQ.1) GO TO 100
C  CALCULATE PERCENT RMS ERROR
   RMS=314.15926*RMS*C/(A*(1.-EXP(-(B*C)**2)))
95 IF(IPRNT.NE.1) RETURN
100 GAMMAC=1.5*A/VINF
   BBAR=B*C
```


ORIGINAL PAGE IS
OF POOR QUALITY

```
E1=100.*SRI2/(VMAXUP+VSINA)
WRITE(6,130) SRI2,E1
130 FORMAT(18X,12HCROSS RMS =,F9.4,9H FT/SEC =,F6.2,9H PER CENT)
140 A1=BBAR/HD
PRINT 150,GAMMAC,GEFF,HD,HEFF,BBAR,A1,VMAXUP
150 FORMAT(/18X,'GAMMAO =',F6.3,4X,'EFFECTIVE GAMMA =',F6.3/18X,
1'H0/D =',F6.3,4X,'EFFECTIVE H/D =',F6.3/18X,'BETA BAR =',
2F6.3,4X,17HBETA ' D =,F6.3/38X,'MAX UPWASH VEL =',F6.2//)
RETURN
999 RMS=C.
RETURN
END
SUBROUTINE PRMAT
COMMON IYZCOD,IYZ,NR,NC,A,B,C,ZO,VINF,VSINA,VY(21,12),VZ(21,12),
1Y(3,12),Z(21),RMS,NDRPF,IPRNT,NPTS,IRMS,RMSVZO(2,5),IPRTM,NRAK
DIMENSION VC(12),CHAR(6),CHR(12)
DATA CHAR/2H ,2H ,2H ,2H$$,1HY,1HZ/
I=4+IYZ
DO 600 J=1,NC
600 VC(J)=12.*Y(1,J)
I1=1.6*RMSVZO(1,1)+0.5
IF(IPRNT.EQ.2) I1=0.1*VINF
IF(I1.LT.1) I1=1
I2=-I1
I3=2*I1
A1=I1
A2=I2
A3=I3
WRITE(6,610) CHAR(I),I1,I2,I3,(VC(J),J=1,NC)
610 FORMAT(///,49X,37HMATRIX OF CROSS-SECTION VELOCITIES//32X,48HCA
1LUCULATED VELOCITIES FROM LEAST SQUARES FIT TO ,A1, 22H COMPONENT O
2F VELOCITY///' Y,Z DENTE Y,Z VELOCITY COMPONENT DATA' ' C DENC
3TES THE CALCULATED VELOCITIES///' INDICATES (V-VCALC) GREATER T
4HAN',I3,'. FT/SEC'/' INDICATES (V-VCALC) LESS THAN',I4,'. FT/S
```

ORIGINAL PAGE IS
OF POOR QUALITY

```
SEC*' '$$ INDICATES ABS(V-VCALC) GREATER THAN',I3,'. FT/SEC.'//1X,13
80(1F*)/3X,4HZ ',51X,'APPROX. Y POSITICNS'/6X,1H*,F7.2,11F10.2)
WRITE(6,620)
620 FORMAT(1X,130(1F*))
C DC LCCP 670 WRITES OUT THE VELOCITY FIELD DATA AND THE VELOCITIES USING FIT
DO 670 I=1,NR
ZW=12.*Z(I)
K=(I+NRPF+6)/7
IYZCCD=1
DO 640 J=1,NC
CHR(J)=CHAR(1)
VC(J)=F(Y(K,J),Z(I))
IF(VY(I,J).GT.1E3) GO TO 640
E1=VY(I,J)-VC(J)
IF(ABS(E1).LT.A1) GO TO 640
IF(ABS(E1).GT.A3) GO TO 630
IF(E1.GT.A1) CHR(J)=CHAR(2)
IF(E1.LT.A2) CHR(J)=CHAR(3)
GO TO 640
630 CHR(J)=CHAR(4)
640 CONTINUE
WRITE(6,680) (VY(I,J),J=1,NC)
WRITE(6,690) (VC(J),CHR(J),J=1,NC)
IYZCCD=2
DO 660 J=1,NC
CHR(J)=CHAR(1)
VC(J)=F(Y(K,J),Z(I))-VSINA
IF(VZ(I,J).GT.1E3) GO TO 660
E1=VZ(I,J)-VC(J)
IF(ABS(E1).LT.A1) GO TO 660
IF(ABS(E1).GT.A3) GO TO 650
IF(E1.GT.A1) CHR(J)=CHAR(2)
IF(E1.LT.A2) CHR(J)=CHAR(3)
GO TO 660
```

```

650 CHR(J)=CHAR(4)
660 CONTINUE
WRITE(6,700) ZW,(VZ(I,J),J=1,NC)
670 WRITE(6,690) (VC(J),CHR(J),J=1,NC)
680 FORMAT(6X,1H*/6X,1H*,12(1X,F6.1,'Y  '))
690 FORMAT(6X,1H*,12(1X,F6.1,'C',A2))
700 FORMAT(F6.2,1H*,12(1X,F6.1,'Z  '))
RETURN
END

```

C FUNCTION F CALCULATES THE VELOCITY INDUCED BY A PAIR OF DISTRIBUTED VORTICES.

```

COMMON IYZCOD,IYZ,NR,NC,A,B,C,ZO
COMMON/DVD/FIB,FIC

```

```
Z=ZZ-ZO
```

```
B2=B*B
```

```
YPC=Y+C
```

```
YMC=Y-C
```

```
R12=Z*Z+YPC*YPC
```

```
R22=Z*Z+YMC*YMC
```

```
IF (R12.EQ.0.) R12=1E-10
```

```
IF (R22.EQ.0.) R22=1E-10
```

```
EXP1=EXP(-B2*R12)
```

```
EXP2=EXP(-B2*R22)
```

```
E1=(1.-EXP1)/R12
```

```
E2=(1.-EXP2)/R22
```

```
IF (R12.LE.1E-10) E1=B2
```

```
IF (R22.LE.1E-10) E2=B2
```

```
IF (IYZCOD.EQ.2) GO TO 1
```

```
F=A*Z*(E2-E1)/6.283185
```

```
RETURN
```

1 F=A*(E1*YPC-E2*YMC)/6.283185

```
RETURN
```

```
ENTRY DF(Y,ZZ)
```

C ENTRY DF CALCULATES THE PARTIAL DERIVATIVES USED IN A DIFFERENTIAL CORRECTION

```

C  METHOD FOR A GAUSSIAN-DISTRIBUTED VORTEX PAIR.
    IF (R12.GT.1E-10) DVH1=2.*YPC*(EXP1*(1.+B2*R12)-1.)/(R12*R12)
    IF (R12.LE.1E-10) DVH1=-2.*YPC*B2*B2
    IF (R22.GT.1E-10) DVH2=2.*YMC*(EXP2*(1.+B2*R22)-1.)/(R22*R22)
    IF (R22.LE.1E-10) DVH2=-2.*YMC*B2*B2
    DF=F/A
    IF (IYZCCD.EQ.2) GO TO 2
    FIB=A*Z*B*(EXP2-EXP1)/3.141593
    FIC=-A*Z*(DVH1+DVH2)/6.283185
    RETURN
2   FIB=A*B*(YPC*EXP1-YMC*EXP2)/3.141593
    FIC=A*(E1+DVH1*YPC+E2+DVH2*YMC)/6.283185
    RETURN
    END
SUBROUTINE AUXIL
C  PERFORMS AUXILIARY OPERATIONS UPON INPUT DATA.
    COMMON IYZCOD,IYZ,NR,NC,A,B,C,ZC,VINF,VSINA,VY(21,12),VZ(21,12),
    IY(3,12),Z(21),RMS,NDRPF,IPRNT,NPTS,IRMS,RMSVZO(2,5),IPRTM,NRAK
    COMMON/ONE/MK,NCDATA,IRUN(4),R,AMJET,X4,Z4,SD,ANGVRT,VRANG
    DIMENSION VC(12)
    DATA AST/1H*/
    IF(IPRTM.EQ.0) GO TO 185
    WRITE(6,150)
150  FORMAT(/10X,'INPUT POSITION DATA')
    DO 170 I=1,NR
    K=(I+NDRPF+6)/7
    WRITE(6,160) (Y(K,J),J=1,NC)
160  FORMAT(/12(F7.2,'Y'))
170  WRITE(6,180) (Z(I),J=1,NC)
180  FORMAT(12(F7.2,'Z'))
C  CCUNT NUMBER OF USABLE DATA POINTS
185  M=NR*NC
    DO 200 I=1,NR
    IF(I.EQ.1 .OR. NRAK.EQ.1) GO TO 190

```



```

      IF(ABS(Z(I)-Z(I-1)).LT..5) M=M-NC
190 DO 200 J=1,NC
      IF(VY(I,J).LT.500.) GO TO 200
      M=M-1
      VY(I,J)=1E6
      VZ(I,J)=1E6
200 CONTINUE
      PRINT 210,M
210 FORMAT(/I4,' DATA POINTS')
      NDATA=M
C PERFORM VORTICITY CALCULATIONS
      A2=0.
      IF(IPRTM.EQ.1) PRINT 220
220 FORMAT(//' VORTICITY CALCULATIONS',10X,24HUNITSO UPPER - ET**2/SEC
1/40X,'LOWER - 1/SEC'/)
      DO 290 I=2,NR
      IF(IPRTM.EQ.1) PRINT 230,(AST,J=1,NC)
230 FORMAT( 5X,12(A1,7X))
      A1=Z(I-1)-Z(I)
      K=(I+NDRPF+6)/7
      L=(I+NDRPF+5)/7
      DO 260 J=2,NC
      IF(VY(I-1,J-1).GT.1E3) GO TO 240
      IF(VY(I ,J-1).GT.1E3) GO TO 240
      IF(VY(I-1,J ) .GT.1E3) GO TO 240
      IF(VY(I ,J ) .LT.1E3) GO TO 250
240 VC(J)=1E6
      GO TO 260
250 VC(J)={(VY(I-1,J-1)-VY(I,J))* (Y(L,J)-Y(K,J-1))+(VY(I-1,J)-VY(I,J-1))
1)* (Y(K,J)-Y(L,J-1))+(VZ(I-1,J-1)+VZ(I,J-1)-VZ(I-1,J)-VZ(I,J))*A1}
2/24.
      A2=A2+VC(J)
260 CONTINUE
      IF(IPRTM.EQ.1) PRINT 270,(VC(J),J=2,NC)

```

ORIGINAL PAGE IS
OF POOR QUALITY

```
270 FORMAT(5X,12(1X,F7.3))
    DO 280 J=2,NC
280 VC(J)=VC(J)*288./ABS(A1*(Y(K,J)+Y(L,J)-Y(K,J-1)-Y(L,J-1)))
    IF(IPRTM.EQ.1) PRINT 300,(VC(J),J=2,NC)
290 CONTINUE
300 FORMAT(5X,12F8.2)
    IF(IPRTM.EQ.1) PRINT 230,(AST,J=1,NC)
    A3=1.5*A2/VINF
    PRINT 310,A2,A3
310 FORMAT(/' SUMMED VORTICITY =',F9.3,21H FT**2/SEC      GAMMA =,F6.3)
C  DO LCCPS 320 AND 330 CONVERT POSITION DATA TO FEET
    DO 320 I=1,NR
320 Z(I)=Z(I)/12.
    ZO=ZO/12.
    DO 330 I=1,NRAK
    DO 330 J=1,NC
330 Y(I,J)=Y(I,J)/12.
    RETURN
    END
    SUBROUTINE QMAJ(NOMR,QMJ,QMN1,QMN2)
C  PURPOSE TO CHOOSE THE MAJOR AND MINOR Q CONDITIONS FOR THE GIVEN VELOCITY RATIO
    QMJ=0.0
    QMN1=0.0
    QMN2=0.0
    GO TO (28,28,21,22,23,24,25,26,28,27),NOMR
21  QMJ=35.9
    QMN1=15.5
    RETURN
22  QMJ=20.2
    QMN1=52.8
    QMN2=8.7
    RETURN
23  QMJ=33.3
    RETURN
```

```

24 GMJ=23.1
   GMN1=35.0
   GMN2=9.1
   RETURN
25 GMJ=26.1
   RETURN
26 GMJ=19.9
   GMN1=12.9
   GMN2=5.1
   RETURN
27 GMJ=12.8
   GMN1=8.2
   GMN2=3.2
28 RETURN
   END

```

```

C   FUNCTION ARCLNG(X,R)
C   PURPOSEC CALCULATE THE ARC LENGTH ALONG THE UNIFIED VORTEX PATH EQUATION,
C   GIVEN X/D AND R.

```

```

   DIMENSION G(8),V(8)
   DATA V/.0950125,.2816035,.4580167,.6178762,.7554044
1, .8656312,.9445750,.9894009/,G/.1894506,.1826034,
2.1691565,.1495959,.1246289,.0951585,.0622535,.0271524/
   DATA E2,A1,A3/2.660516,.4633684,-1.141726/
   E3=.1414484*R**2.253072*X**A3
   S=0.
   DO 1 I=1,8
1  S=S+G(I)*{SQRT((1.+V(I))**E2+E3) + SQRT((1.-V(I))**E2+E3)}
   ARCLNG=A1*X*S
   RETURN
   END

```

```

C   SUBROUTINE MINV3(A,D)
C   PURPOSEC PERFORM MATRIX INVERSE OF NORMAL EQUATION MATRIX FROM LEAST SQUARES.
   DIMENSION A(6),B(3)
   REAL*8 A,B,C,D

```

```
B(1)=A(3)*A(5)-A(4)*A(4)
B(2)=A(3)*A(4)-A(2)*A(5)
B(3)=A(2)*A(4)-A(3)*A(3)
C=A(1)*B(1)+A(2)*B(2)+A(3)*B(3)
IF(C.EQ.0.) RETURN
C  =(A(1)*A(5)-A(3)*A(3))/C
A(5)=(A(2)*A(3)-A(1)*A(4))/C
A(6)=(A(1)*A(3)-A(2)*A(2))/C
A(1)=B(1)/D
A(2)=B(2)/D
A(3)=B(3)/D
A(4)=C
RETURN
END
```

REFERENCES

1. Fearn, R. and Weston, R., "Vorticity Associated with a Jet in a Cross Flow," AIAA Journal, Vol. 12, No. 12, Dec. 1974, pp. 1666-1671.
2. Kamotani, Y. and Greber, I., "Experiments on a Turbulent Jet in a Cross Flow," AIAA Journal, Vol. 10, No. 11, Nov. 1972, pp. 1425-1429.
3. Harms, L., Experimental Investigation of the Flow Field of a Hot Turbulent Jet with Lateral Flow, Part II. NASA TT F-15, 706, 1974.
4. Thompson, A. M., "The Flow Induced by Jet Exhausting Normally from a Plane Wall into a Airstream," Ph.D. Thesis, Univ. of London, London, England (Sept. 1971).
5. Fearn, R. and Weston, R., "A Jet in a Cross Flow - The Induced Pressure Distribution. NASA TN D, to be published.
6. Pratte, B. D. and Baines, W. D., "Profiles of the Round Turbulent Jet in a Cross Flow," Journal of the Hydraulics Division, Proceedings of the ASCE, Vol. 92, No. HY6, Nov. 1967, pp. 53-64.
7. Chang-Lu, H., "Aufrollung eines Zylindrischen Strahles durch Querwind," Ph.D. Dissertation, Univ. of Gottingen, Gottingen, F. R., Germany, 1942.
8. Fearn, R., Unpublished Research Notes, April. 1974.
9. Nielsen, K. L., Methods in Numerical Analysis, 2nd ed. Macmillan, New York, 1964, pp. 308-311.
10. Calter, P., Problem Solving with Computers, McGraw-Hill Inc. New York, 1973, pp. 101-106.

BIOGRAPHICAL SKETCH

William L. Sellers III was born [REDACTED].

The family moved to Cocoa Beach, Florida where William graduated from Cocoa Beach High School in 1965. He entered Brevard Junior College in Cocoa, Florida and received the degree of Associate of Arts in 1968. William entered active duty with the United States Navy for a period of 2 years in which he served on the staff of the Commander, Naval Air Forces, U.S. Atlantic Fleet in Norfolk, Virginia. While on active duty with the U.S. Navy, he attended Old Dominion University in Norfolk, Virginia. After completion of his active military service, he entered the University of Florida and received the degree of Bachelor of Science in Aerospace Engineering in August, 1973. He entered the graduate school of the University of Florida and is scheduled to complete the Master's program in March, 1975.

I certify that I have read this study and that in my opinion it conforms to acceptable standards of scholarly presentation and is fully adequate, in scope and quality, as a thesis for the degree of Master of Science in Engineering.

Richard L. Fearn

Richard L. Fearn, Chairman
Assistant Professor of
Engineering Sciences

I certify that I have read this study and that in my opinion it conforms to acceptable standards of scholarly presentation and is fully adequate, in scope and quality, as a thesis for the degree of Master of Science in Engineering.

D. Max Sheppard

D. Max Sheppard
Assistant Professor of
Engineering Sciences

I certify that I have read this study and that in my opinion it conforms to acceptable standards of scholarly presentation and is fully adequate, in scope and quality, as a thesis for the degree of Master of Science in Engineering.

R. A. Gater

Roger A. Gater
Associate Professor of
Mechanical Engineering

This thesis was submitted to the Graduate Faculty of the College of Engineering and to the Graduate Council, and was accepted as partial fulfillment of the requirements for the degree of Master of Science in Engineering.

March, 1975

Dean, College of Engineering

Dean, Graduate School